Collisionless kinetic-fluid model of zonal flows in toroidal plasmas

H. Sugama and T.-H. Watanabe
National Institute for Fusion Science, Graduate University for Advanced Studies, Toki 509-5292, Japan
W. Horton
Institute for Fusion Studies, The University of Texas at Austin, Austin, Texas 78712

(Received 10 November 2006; accepted 2 January 2007; published online 7 February 2007)

A novel kinetic-fluid model is presented, which describes collisionless time evolution of zonal flows in tokamaks. In the new zonal-flow closure relations, the parallel heat fluxes are written by the sum of short- and long-time-evolution parts. The former part is given in the dissipative form of the parallel heat diffusion and relates to collisionless damping processes. The latter is derived from the long-time-averaged gyrocenter distribution and plays a major role in describing low-frequency or stationary zonal flows, for which the parallel heat fluxes are expressed in terms of the parallel flow as well as the nonlinear-source and initial-condition terms. It is shown analytically and numerically that, when applied to the zonal flow driven by either ion or electron temperature gradient turbulence, the kinetic-fluid equations including the new closure relations can reproduce the same long-time zonal-flow responses to the initial condition and to the turbulence source as those obtained from the gyrokinetic model. © *2007 American Institute of Physics*. [DOI: 10.1063/1.2435329]

I. INTRODUCTION

In recent years, favorable effects of $\mathbf{E}\times\mathbf{B}$ zonal flows on plasma confinement have been well recognized from numerous theories, simulations, and experiments on turbulent transport.[1,2] One branch of zonal flows occurs as dynamical oscillations of the radial electric field and is called the geodesic acoustic mode (GAM).[3] The GAM is caused by compressibility of the $\mathbf{E}\times\mathbf{B}$ drift velocity in the presence of the geodesic magnetic curvature and the GAM oscillations are experimentally observed in many toroidal devices.[2,4,5] Another branch of zonal flows appears in the low-frequency regime or as a stationary flow with oscillatory structures in the radial direction, which can reduce turbulent transport driven by microinstabilites such as ion temperature gradient (ITG) modes[6] while the turbulence itself generates the zonal flow.

Collisionless time evolution processes of zonal flows in the ITG turbulence were analytically investigated by Rosenbluth and Hinton[7] for tokamaks and by Sugama and Watanabe[8,9] for helical systems based on the gyrokinetic theory. These theoretical studies showed and subsequent gyrokinetic simulations[10,11] verified that initial $\mathbf{E}\times\mathbf{B}$ rotation is not fully damped by collisionless processes but it approaches the stationary zonal-flow state with a finite amplitude of the radial electric field after the GAM oscillation is Landau damped. The relative magnitude of this residual zonal flow measures how efficiently the zonal flow is produced by the turbulence source or how effectively the turbulence is suppressed by the zonal flow. Thus, an accurate theoretical description of the long-time zonal-flow evolution is a key issue for correctly predicting the turbulent transport of fusion plasmas. In fact, unless the residual zonal flow is properly treated in a gyrofluid model, the gyrofluid simulation cannot reproduce the same turbulent transport as given by the gyrokinetic simulation.[7,10,12] Thus, fast and satisfactory evaluations of the turbulent transport coefficients based on the gyrofluid simulation greatly depend on establishing a reliable closure model for zonal modes or $n=0$ modes where n denotes the toroidal mode number. The importance of the zonal-flow treatment is also acknowledged from gyrokinetic simulation results showing that characteristics of the electron temperature gradient (ETG) turbulence are strikingly different from those of the ITG turbulence because of a change in the zonal-flow mechanism.[13] When the Debye length is neglected, the governing equations for the ITG turbulence with no trapped-electron effects are symmetric to those for the ETG turbulence except that equations for the flux-surface-averaged electrostatic potential in the two cases are asymmetric to each other.

In the present paper, we investigate how to correctly express collisionless zonal-flow evolution in the tokamak ITG and ETG turbulence by using a kinetic-fluid model. First, the long-time responses of zonal flows to the initial perturbed distribution function and to the turbulence source terms are comprehensively described based on the analytic solution of the gyrokinetic equation in Sec. II. As for the residual zonal flow in the wave number region relevant to either ITG or ETG turbulence, we explicitly discuss the incompressibility condition and the initial-parallel-flow dependence, which were not fully remarked in previous works. Also, our formula for the ETG-mode-driven zonal flow contains a new correction term missed in the work by Kim *et al.*[14]

In Sec. III, by making the best use of the above-mentioned gyrokinetic-analysis results, the main purpose of this work, derivation of the kinetic-fluid model to describe the collisionless zonal-flow evolution, is carried out. In our previous works,[15,16] the nondissipative closure model (NCM) was constructed and successfully applied to the kinetic-fluid simulation of the slab ITG turbulence, which gave about the same turbulent ion heat transport as that obtained from the direct kinetic turbulence simulation although these works were limited to the cases with no zonal flows. In our novel zonal-flow closure model, the parallel heat fluxes consist of the short- and long-time-evolution parts, in which the former part is written in the dissipative parallel-diffusion form of the Hammett-Perkins-type[17] while the latter takes the nondissipative form determined from the analytically derived gyrocenter distribution. Compared with the zonal-flow closure model by Beer and Hammett,[12] our model is different from theirs in that we use the parallel flow as well as the nonlinear-source and initial-condition terms to represent the parallel heat fluxes. Using this representation allows us to analytically show that the same response formulas for the ITG- and ETG-mode-driven zonal flows as those derived kinetically in Sec. II are obtained from the kinetic-fluid equations as well.

In Sec. IV, for further confirmation of the validity of the closure model, the ITG and ETG zonal-flow response functions are obtained from numerical solutions of the kinetic-fluid equations and compared with gyrokinetic simulation results. Finally, conclusions are given in Sec. V. The successful analytical and numerical validity checks make our model promising for future applications to kinetic-fluid turbulence simulations for prediction of the turbulent transport as well as to theoretical studies of zonal-flow physics. In Appendix A, useful formulas for the incompressible zonal flow are shown. Appendices B and C present kinetic-fluid equations of ITG-mode-driven zonal flows in large-aspect-ratio tokamaks and those of ETG-mode-driven zonal flows, respectively. Appendix D shows the GAM dispersion relation derived from the kinetic-fluid model.

II. KINETIC DESCRIPTION OF ZONAL FLOWS

In this section, gyrokinetic and Poisson's equations to govern the zonal-flow dynamics are shown and long-time behaviors of ITG- and ETG-mode-driven zonal flows in tokamaks are described in detail by using the analytic solution of the gyrokinetic equation.

A. Basic equations

The collisionless gyrokinetic equation[18] for the zonal-flow component with the perpendicular wave number vector $\mathbf{k}_\perp = k_r \nabla r$ (r: the radial coordinate to label flux surfaces) is given in terms of the perturbed *gyrocenter* distribution function $\delta f^{(g)}_{\mathbf{k}_\perp}$ by

$$\left(\frac{\partial}{\partial t} + v_\parallel \mathbf{b}\cdot\nabla + i\omega_D\right)\delta f^{(g)}_{\mathbf{k}_\perp} = -(v_\parallel \mathbf{b}\cdot\nabla + i\omega_D)\left(F_0 J_0(k_\perp\rho)\frac{e\phi_{\mathbf{k}_\perp}}{T}\right) + S_{\mathbf{k}_\perp}F_0, \quad (1)$$

where F_0 is the local equilibrium distribution function that takes the Maxwellian form, $J_0(k_\perp\rho)$ is the zeroth-order Bessel function, $\rho = v_\perp/\Omega$ is the gyroradius, $\Omega = eB/(mc)$ is the gyrofrequency, and $\mathbf{b} = \mathbf{B}/B$ is the unit vector along the magnetic field line. Here, subscripts to represent particle species are dropped for simplicity. In Eq. (1), $\delta f^{(g)}_{\mathbf{k}_\perp}$ is regarded as a function of independent variables (θ, w, μ), where $w \equiv \frac{1}{2}mv^2$ and $\mu \equiv mv_\perp^2/(2B)$ represent the kinetic energy and the magnetic moment, respectively, and the ballooning representation[19,20] is employed to use the poloidal angle θ as a coordinate along the field line. The drift frequency ω_D is defined by $\omega_D \equiv \mathbf{k}_\perp \cdot \mathbf{v}_d$, where $\mathbf{v}_d$ is the gyrocenter-drift velocity. The source term $S_{\mathbf{k}_\perp}F_0$ on the right-hand side of Eq. (1) represents the $\mathbf{E}\times\mathbf{B}$ nonlinearity and is written as $S_{\mathbf{k}_\perp}F_0 = (c/B)\Sigma_{\mathbf{k}'_\perp + \mathbf{k}''_\perp = \mathbf{k}_\perp}[\mathbf{b}\cdot(\mathbf{k}'_\perp \times \mathbf{k}''_\perp)]J_0(k'_\perp\rho)\phi_{\mathbf{k}'_\perp}\delta f^{(g)}_{\mathbf{k}''_\perp}$.

The perturbed *particle* distribution function $\delta f_{\mathbf{k}_\perp}$ is written in terms of the perturbed gyrocenter distribution function $\delta f^{(g)}_{\mathbf{k}_\perp}$ and the electrostatic potential $\phi_{\mathbf{k}_\perp}$ as

$$\delta f_{\mathbf{k}_\perp} = \delta f^{(g)}_{\mathbf{k}_\perp} e^{-i\mathbf{k}_\perp\cdot\boldsymbol{\rho}} - \frac{e\phi_{\mathbf{k}_\perp}}{T}F_0[1 - J_0(k_\perp\rho)e^{-i\mathbf{k}_\perp\cdot\boldsymbol{\rho}}], \quad (2)$$

where $\boldsymbol{\rho} = \mathbf{b}\times\mathbf{v}/\Omega$. Hereafter, the equilibrium density, temperature, and pressure are denoted by n_0, T, and $p_0 \equiv n_0 T$, respectively. On the right-hand side of Eq. (2), the factor $e^{-i\mathbf{k}_\perp\cdot\boldsymbol{\rho}}$ in the first term results from the difference between the particle and gyrocenter positions while the second group of terms represent the polarization, that is the variation of the particle distribution due to the potential perturbation.

The electrostatic potential $\phi_{\mathbf{k}_\perp}$ is determined by Poisson's equation,

$$\int d^3v J_0 f^{(g)}_{i\mathbf{k}_\perp} - n_0\frac{e\phi_{\mathbf{k}_\perp}}{T_i}[1 - \Gamma_0(b_i)] - \int d^3v J_0 f^{(g)}_{e\mathbf{k}_\perp} - n_0\frac{e\phi_{\mathbf{k}_\perp}}{T_e}[1 - \Gamma_0(b_e)] = n_0\frac{e\phi_{\mathbf{k}_\perp}}{T_e}(k_\perp\lambda_{\mathrm{De}})^2, \quad (3)$$

where the subscripts representing ions (i) and electrons (e) are explicitly shown. In Eq. (3), $\lambda_{\mathrm{De}} \equiv T_e/(4\pi n_0 e^2)$ is the electron Debye length, $b_a \equiv k_\perp^2 T_a/(m_a\Omega_a)$, and $\Gamma_0(b_a) \equiv I_0(b_a)e^{-b_a}$ $(a = i, e)$, where I_0 denotes the zeroth-order modified Bessel function.

When the initial gyrocenter distribution functions $\delta f^{(g)}_{a\mathbf{k}_\perp}(t=0)$ and the past history of the source terms $S_{a\mathbf{k}_\perp}(t')$ $(a = i, e)$ are given, the gyrocenter distribution functions $\delta f^{(g)}_{a\mathbf{k}_\perp}(t)$ at an arbitrary time $t > 0$ are determined by solving Eqs. (1) and (3) [note that the initial potential $\phi_{\mathbf{k}_\perp}(t=0)$ is immediately given in terms of $\delta f^{(g)}_{a\mathbf{k}_\perp}(t=0)$ by using Eq. (3)]. Examining properties of these equations, we find that, in the static magnetic field, the response of $\delta f^{(g)}_{a\mathbf{k}_\perp}(t)$ to $\delta f^{(g)}_{a'\mathbf{k}_\perp}(t=0)$ and $S_{a'\mathbf{k}_\perp}(t')$ $(a, a' = i, e;\ 0 \le t' \le t)$ should take the form,

$$\delta f^{(g)}_{a\mathbf{k}_\perp}(t) = \sum_{a'=i,e}\left[U_{aa'}(t)\delta f^{(g)}_{a'\mathbf{k}_\perp}(0) + \int_0^t dt'\, U_{aa'}(t-t')F_{a'0}S_{a'\mathbf{k}_\perp}(t')\right]. \quad (4)$$

Here, it should be noted that, once the linear operators (or propagators) $U_{aa'}(t)$ $(a, a' = i, e)$, which relate $\delta f^{(g)}_{a\mathbf{k}_\perp}(t)$ to

$\delta f^{(g)}_{a'\mathbf{k}_\perp}(0)$, are known, we can immediately obtain the kernels in the time integration representing the response to $F_{a'0}S_{a'\mathbf{k}_\perp}(t')$ by replacing the time argument t with $t-t'$. In other words, the solution of the linear initial-value problem is equivalent to the linear responses to the source terms. Substituting Eq. (4) into Eq. (3), we have

$$\frac{e\phi_{\mathbf{k}_\perp}(t)}{T_i} = \frac{1}{n_0}\sum_{a=i,e}\left[N_a(t)\delta f^{(g)}_{a\mathbf{k}_\perp}(0) + \int_0^t dt' N_a(t-t')F_{a0}S_{a\mathbf{k}_\perp}(t')\right] \times\{[1-\Gamma_0(b_i)] + (T_i/T_e)[1-\Gamma_0(b_e) + (k_\perp\lambda_{\mathrm{De}})^2]\}^{-1}, \tag{5}$$

where $N_a(t)\equiv\int d^3v J_0(k_\perp\rho_i)U_{ia}(t) - \int d^3v J_0(k_\perp\rho_e)U_{ea}(t)$.

B. Axisymmetric geometry

Equations (1)–(5) shown above are valid for general magnetic configurations although we hereafter consider only axisymmetric toroidal systems, in which the magnetic field is written as

$$\mathbf{B} = I(r)\nabla\zeta + \nabla\zeta\times\nabla\psi(r) = \mathbf{B}_t + \mathbf{B}_p. \tag{6}$$

Here, the toroidal coordinates (r,θ,ζ) are used, where θ and ζ represent the poloidal and toroidal angles, respectively. The toroidal and poloidal fields are represented by $\mathbf{B}_t = I\nabla\zeta$ and $\mathbf{B}_p = \nabla\zeta\times\nabla\psi$, respectively, and thus their magnitudes are given by $B_t = |\mathbf{B}_t| = I/R$ and $B_p = |\mathbf{B}_p| = |\nabla\psi|/R$, respectively, where R is the major radius. The poloidal flux within the flux surface labeled r is given by $2\pi\psi(r)$ and the safety factor is denoted by $q(r)$.

For the axisymmetric case, we find[7]

$$i\omega_D = ik_r\mathbf{v}_d\cdot\nabla r = iv_\parallel\mathbf{b}\cdot\nabla Q = e^{-iQ}v_\parallel\mathbf{b}\cdot\nabla e^{iQ}. \tag{7}$$

Here, $Q\equiv Kv_\parallel/B$ measures the radial orbit width normalized by the radial wavelength, where $K\equiv(mc/e)k_r I/(d\psi/dr) = k_\perp B_t/\Omega_p$, $\Omega_p\equiv eB_p/(mc)$, and $\mathbf{b}\cdot\nabla K = 0$. Multiplying both sides of Eqs. (1) with e^{iQ} and using (7) yield

$$\left(\frac{\partial}{\partial t} + v_\parallel\mathbf{b}\cdot\nabla\right)(e^{iQ}\delta f^{(g)}_{\mathbf{k}_\perp}) = -v_\parallel\mathbf{b}\cdot\nabla\left(e^{iQ}F_0 J_0(k_\perp\rho)\frac{e\phi_{\mathbf{k}_\perp}}{T}\right) + e^{iQ}S_{\mathbf{k}_\perp}F_0. \tag{8}$$

Integrating Eq. (8) over the velocity space and taking its flux-surface average, we obtain

$$\frac{\partial}{\partial t}\left\langle\int d^3v e^{iQ}\delta f^{(g)}_{\mathbf{k}_\perp}\right\rangle = \left\langle\int d^3v e^{iQ}S_{\mathbf{k}_\perp}F_0\right\rangle, \tag{9}$$

where $\langle\cdot\rangle$ denotes the flux-surface average. For small radial wave numbers, we use $e^{iQ} = 1 + iQ - \frac{1}{2}Q^2 + \cdots$ to approximately rewrite Eq. (9) as

$$\frac{\partial}{\partial t}\left\langle\delta n^{(g)}_{\mathbf{k}_\perp} + i\left(\frac{K}{B}\right)n_0 u_{\parallel\mathbf{k}_\perp} - \left(\frac{K}{B}\right)^2\frac{\delta p_{\parallel\mathbf{k}_\perp}}{2m}\right\rangle = \left\langle\int d^3v\left(1 + iQ - \frac{1}{2}Q^2\right)S_{\mathbf{k}_\perp}F_0\right\rangle, \tag{10}$$

where the perturbed gyrocenter density, the parallel flow, and the perturbed parallel pressure are defined by $\delta n^{(g)}_{\mathbf{k}_\perp} \equiv \int d^3v\,\delta f^{(g)}_{\mathbf{k}_\perp}$, $u_{\parallel\mathbf{k}_\perp} \equiv n_0^{-1}\int d^3v\,\delta f^{(g)}_{\mathbf{k}_\perp}v_\parallel$, and $\delta p_{\parallel\mathbf{k}_\perp} \equiv \int d^3v\,\delta f^{(g)}_{\mathbf{k}_\perp}mv_\parallel^2$, respectively. We will see later that Eq. (10) is useful in deriving important formulas for zonal flows in axisymmetric systems.

C. Long-time evolution of zonal flows

Considering the long-time evolution of the perturbed gyrocenter distribution function with characteristic frequencies much lower than the bounce frequency ($|\partial/\partial t| \ll |v_\parallel\mathbf{b}\cdot\nabla|$), Eq. (8) is perturbatively solved to give the lowest-order solution as[7]

$$\delta f^{(g)}_{\mathbf{k}_\perp} = -J_0(k_\perp\rho)\frac{e\phi_{\mathbf{k}_\perp}}{T}F_0 + he^{-iQ}, \tag{11}$$

where $\mathbf{b}\cdot\nabla h = 0$ and

$$h(t) = \overline{[e^{iQ}\delta f^{(g)}_{\mathbf{k}_\perp}(0)]} + F_0\overline{\{e^{iQ}[J_0 e\phi_{\mathbf{k}_\perp}(t)/T + R_{\mathbf{k}_\perp}(t)]\}}. \tag{12}$$

Here, $R_{\mathbf{k}_\perp}(t) \equiv \int_0^t dt' S_{\mathbf{k}_\perp}(t')$ and

$$\overline{(e^{iQ}\delta f^{(g)}_{\mathbf{k}_\perp})} = -\frac{e}{T}F_0\overline{(e^{iQ}J_0\phi_{\mathbf{k}_\perp})} + h \tag{13}$$

are used. Here, the orbital average is denoted by $\overline{\cdots} \equiv \oint(dl/v_\parallel)\cdots/\oint(dl/v_\parallel)$, where dl represents the line element along the field line and the integral goes over a closed orbit for trapped particles but once around the poloidal circumference for passing particles. Substituting Eq. (12) into Eq. (11), we obtain

$$\delta f^{(g)}_{\mathbf{k}_\perp}(t) = -\frac{e}{T}F_0\{J_0\phi_{\mathbf{k}_\perp}(t) - e^{-iQ}\overline{[e^{iQ}J_0\phi_{\mathbf{k}_\perp}(t)]}\} + e^{-iQ}\overline{\{e^{iQ}[\delta f^{(g)}_{\mathbf{k}_\perp}(0) + F_0 R_{\mathbf{k}_\perp}(t)]\}}. \tag{14}$$

Now, assuming that $k_\perp\rho \ll 1$ and that $\phi_{\mathbf{k}_\perp}$ is constant on the flux surface, i.e., $\phi_{\mathbf{k}_\perp} = \langle\phi_{\mathbf{k}_\perp}\rangle$, Eq. (14) is written as

$$\delta f_{\mathbf{k}_\perp}^{(g)}(t) = F_0 \frac{e\phi_{\mathbf{k}_\perp}(t)}{T}\left\{ - iK[(v_\parallel/B) - \overline{(v_\parallel/B)}] + K^2\left[(v_\parallel/B)\overline{(v_\parallel/B)} - \frac{1}{2}(v_\parallel/B)^2 - \frac{1}{2}\overline{(v_\parallel/B)^2}\right] + \frac{1}{4}[(k_\perp\rho)^2 - \overline{(k_\perp\rho)^2}]\right\} + \overline{\delta f_{\mathbf{k}_\perp}^{(g)}(0)}$$
$$+ F_0\overline{R_{\mathbf{k}_\perp}(t)} - iK((v_\parallel/B)[\overline{\delta f_{\mathbf{k}_\perp}^{(g)}(0)} + F_0\overline{R_{\mathbf{k}_\perp}(t)}] - \overline{\{(v_\parallel/B)[\delta f_{\mathbf{k}_\perp}^{(g)}(0) + F_0R_{\mathbf{k}_\perp}(t)]\}})$$
$$+ K^2\left[(v_\parallel/B)\overline{\{(v_\parallel/B)[\delta f_{\mathbf{k}_\perp}^{(g)}(0) + F_0R_{\mathbf{k}_\perp}(t)]\}} - \frac{1}{2}(v_\parallel/B)^2[\overline{\delta f_{\mathbf{k}_\perp}^{(g)}(0)} + F_0\overline{R_{\mathbf{k}_\perp}(t)}] - \frac{1}{2}\overline{\{(v_\parallel/B)^2[\delta f_{\mathbf{k}_\perp}^{(g)}(0) + F_0R_{\mathbf{k}_\perp}(t)]\}}\right], \tag{15}$$

where $J_0(k_\perp\rho)=1-\frac{1}{4}(k_\perp\rho)^2+\cdots$ and $e^{iQ}=1+iKv_\parallel/B-\frac{1}{2}(Kv_\parallel/B)^2+\cdots$ are used. As shown in Appendix A, the perturbed gyrocenter distribution function given by Eq. (15) indicates the incompressibility of zonal flows in the long-time evolution, where fast compressional waves such as GAMS are ignored.

1. Residual zonal flows in ITG turbulence

Here, we treat residual zonal flows in the ITG turbulence which were originally investigated by Rosenbluth and Hinton.[7] Let us consider the wave-number region relevant to the ITG turbulence and take $k_\perp a_i < 1$ where $a_i \equiv (T_i/m_i)^{1/2}/\Omega_i$. Then, in Eq. (3), we put $1-\Gamma_0(b_i)\simeq b_i \equiv k_\perp^2 a_i^2$, $1-\Gamma_0(b_e)\simeq 0$, $k_\perp\lambda_{\rm De}\simeq 0$, and neglect the perturbed electron density $\delta n_e \simeq \int d^3v J_0 \delta f_{e\mathbf{k}_\perp}^{(g)}$ which is much smaller than the perturbed ion density because of the small mass ratio m_e/m_i as verified also from Eq. (15). Now, Eq. (3) is approximately rewritten as

$$\delta n_{i\mathbf{k}_\perp}^{(g)}(t) = n_0(k_\perp^2 a_i^2)(e\phi_{\mathbf{k}_\perp}(t)/T_i) \tag{16}$$

where $\delta n_{i\mathbf{k}_\perp}^{(g)}(t) \equiv \int d^3v\, \delta f_{i\mathbf{k}_\perp}^{(g)}(t)$ represents the perturbed ion gyrocenter density. We find from Eq. (16) that, in Eq. (A4), the density-gradient-driven drift is smaller than the $\mathbf{E}\times\mathbf{B}$ drift by a factor of $k_\perp^2 a_i^2 \ll 1$ so that the perpendicular ion flow is written as $u_{i\perp\mathbf{k}_\perp} = ick_\perp \phi_{i*\mathbf{k}_\perp}/B \simeq ick_\perp\phi_{\mathbf{k}_\perp}/B$. Substituting Eq. (16) into Eq. (10), taking its time integral, and neglecting terms of higher-order in $k_\perp a_i$, the balance equation of the flux-surface-averaged ion toroidal angular momentum (per unit mass) is obtained as

$$\langle Ru_{it\mathbf{k}_\perp}(t)\rangle - \langle Ru_{it\mathbf{k}_\perp}(0)\rangle = \langle R[B_t u_{i\parallel\mathbf{k}_\perp}^{(s)}(t) - B_p u_{i\perp\mathbf{k}_\perp}^{(s)}(t)]/B\rangle$$
$$\equiv \langle Ru_{it\mathbf{k}_\perp}^{(s)}(t)\rangle, \tag{17}$$

where the toroidal flow $u_{it\mathbf{k}_\perp}$ is defined by Eq. (A3), and

$$u_{i\parallel\mathbf{k}_\perp}^{(s)}(t) \equiv \frac{1}{n_0}\int d^3v F_{i0} R_{i\mathbf{k}_\perp}(t) v_\parallel,$$

$$u_{i\perp\mathbf{k}_\perp}^{(s)}(t) \equiv \frac{ick_\perp\phi_{\mathbf{k}_\perp}^{(s)}(t)}{B} \equiv \frac{ick_\perp\langle\delta n_{i\mathbf{k}_\perp}^{(s)}(t)\rangle}{n_0 B\langle k_\perp^2 a_i^2\rangle(e/T_i)}$$
$$\equiv \frac{ick_\perp}{n_0 B\langle k_\perp^2 a_i^2\rangle(e/T_i)}\left\langle \int d^3v F_{i0}R_{i\mathbf{k}_\perp}(t)\right\rangle \tag{18}$$

are used. In Eqs. (17) and (18), $u_{i\parallel\mathbf{k}_\perp}^{(s)}(t)$, $u_{i\perp\mathbf{k}_\perp}^{(s)}(t)$, and $u_{it\mathbf{k}_\perp}^{(s)}(t)$ represent the sources of the parallel, perpendicular, and toroidal flows associated with the turbulence, respectively. Similarly, $\phi_{\mathbf{k}_\perp}^{(s)}(t)$ and $\delta n_{i\mathbf{k}_\perp}^{(s)}(t)$ denote the turbulent sources of the electrostatic potential and the perturbed ion gyrocenter density, respectively. The definition of $u_{i\parallel\mathbf{k}_\parallel}^{(s)}(t)$ in Eq. (18) is consistent with the same notation used in Eq. (A15) for the case, in which the turbulence source takes the form of the shifted Maxwellian. When there is no turbulence source, Eq. (17) results in the toroidal angular momentum conservation, $\langle Ru_{it\mathbf{k}_\perp}(t)\rangle = \langle Ru_{it\mathbf{k}_\perp}(0)\rangle$.

Substituting Eq. (15) for ions into $\delta n_{i\mathbf{k}_\perp}^{(g)}(t) \equiv \int d^3v\, \delta f_{i\mathbf{k}_\perp}^{(g)}(t)$ in Eq. (16) and taking its flux-surface average, we obtain

$$\frac{e\phi_{\mathbf{k}_\perp}(t)}{T_i} = \frac{1}{\mathcal{D}_{\rm ITG}}\left\langle \int d^3v\{1 + iK_i[(v_\parallel/B) - \overline{(v_\parallel/B)}]\}\right.$$
$$\left. \times \{\delta f_{i\mathbf{k}_\perp}^{(g)}(0) + F_{i0}R_{i\mathbf{k}_\perp}(t)\}\right\rangle, \tag{19}$$

where

$$\mathcal{D}_{\rm ITG} \equiv n_0\langle k_\perp^2 a_i^2\rangle + \left\langle \int d^3v F_{i0}K_i^2[\overline{(v_\parallel/B)^2} - (\overline{v_\parallel/B})^2]\right\rangle$$
$$= n_0\left[\langle k_\perp^2 a_i^2\rangle + K_i^2\frac{T_i}{m_i}(\langle B^{-2}\rangle - \beta_1)\right]$$
$$= n_0\langle k_\perp^2 a_{ip}^2(1-\beta_1 B_t^2)\rangle. \tag{20}$$

Here, $a_{ip}\equiv (T_i/m_i)^{1/2}/\Omega_{ip}$ represents the ion poloidal gyroradius, $\Omega_{ip}\equiv eB_p/(m_i c)$ is the poloidal gyrofrequency, and

$$\beta_1 \equiv \frac{3}{2}\int_0^{1/B_M} \frac{d\lambda}{\langle B/(1-\lambda B)^{1/2}\rangle}, \tag{21}$$

where B_M denotes the maximum field strength over the flux surface. On the right-hand side of the first line in Eq. (20), the first term represents the shielding effect of the classical ion polarization while the second integral terms, which are proportional to $K_i^2 \equiv (k_\perp B_t/\Omega_{ip})^2$, correspond to the neoclassical polarization effect due to trapped ions. In contrast to Rosenbluth and Hinton,[7] the initial distribution $\delta f_{i\mathbf{k}_\perp}^{(g)}(0)$ is explicitly shown in Eq. (19) instead of including it into the source term $F_{i0}R_{i\mathbf{k}_\perp}(t)$. When we use Eqs. (A14) and (A15), Eq. (19) is rewritten as

$$\frac{e\phi_{\mathbf{k}_\perp}(t)}{T_i} = \frac{n_0}{\mathcal{D}_{\rm ITG}}\left[\langle k_\perp^2 a_i^2\rangle \frac{e\phi_{\mathbf{k}_\perp}(0)}{T_i} + \frac{\langle \delta n_{i\mathbf{k}_\perp}^{(s)}(t)\rangle}{n_0} + iK_i(\langle\{u_{i\parallel\mathbf{k}_\perp}(0)+u_{i\parallel\mathbf{k}_\perp}^{(s)}(t)\}/B\rangle - \beta_1\langle\{u_{i\parallel\mathbf{k}_\perp}(0)+u_{i\parallel\mathbf{k}_\perp}^{(s)}(t)\}B\rangle)\right]$$
$$= \frac{e\phi_{\mathbf{k}_\perp}(0)}{T_i} + i\frac{n_0K_i}{\mathcal{D}_{\rm ITG}}[\langle\{u_{ip\mathbf{k}_\perp}(0)+u_{ip\mathbf{k}_\perp}^{(s)}(t)\}/B_p\rangle - \beta_1\langle B^2\{u_{ip\mathbf{k}_\perp}(0)+u_{ip\mathbf{k}_\perp}^{(s)}(t)\}/B_p\rangle], \tag{22}$$

where $u_{ip\mathbf{k}_\perp}^{(s)}(t)$ is defined by $u_{ip\mathbf{k}_\perp}^{(s)}(t)=[B_p u_{i\parallel\mathbf{k}_\perp}^{(s)}(t)+B_t u_{i\perp\mathbf{k}_\perp}^{(s)}(t)]/B$ and Eq. (18). In deriving Eq. (22), $\phi_{\mathbf{k}_\perp}(0)$ as well as $\phi_{\mathbf{k}_\perp}(t)$ is assumed to be constant on the flux surface while $u_{i\parallel\mathbf{k}_\perp}(0)$ is not. Dependence of the perpendicular long-time zonal-flow component $u_{i\perp\mathbf{k}_\perp}(t)$ on the initial condition and the turbulence source is given by $u_{i\perp\mathbf{k}_\perp}(t)=ick_\perp\phi_{\mathbf{k}_\perp}(t)/B$ with Eq. (22). Substituting Eq. (22) into Eq. (A8) and using Eqs. (A17) and (A2), we have the ion poloidal zonal-flow component as

$$u_{ip\mathbf{k}_\perp}(t)/B_p = \frac{n_0\beta_1}{\mathcal{D}_{\rm ITG}}\Bigg[iK_i\frac{T_i}{m_i}\left(\langle k_\perp^2 a_i^2\rangle\frac{e\phi_{\mathbf{k}_\perp}(0)}{T_i} + \frac{\langle \delta n_{i\mathbf{k}_\perp}^{(s)}(t)\rangle}{n_0}\right) + \left(\langle k_\perp^2 a_i^2\rangle + K_i^2\frac{T_i}{m_i}\langle B^{-2}\rangle\right)$$
$$\times\langle\{u_{i\parallel\mathbf{k}_\perp}(0)+u_{i\parallel\mathbf{k}_\perp}^{(s)}(t)\}B\rangle - K_i^2\frac{T_i}{m_i}\langle\{u_{i\parallel\mathbf{k}_\perp}(0)+u_{i\parallel\mathbf{k}_\perp}^{(s)}(t)\}/B\rangle\Bigg]$$
$$= \frac{n_0\beta_1}{\mathcal{D}_{\rm ITG}}\left[\left(\langle k_\perp^2 a_i^2\rangle + K_i^2\frac{T_i}{m_i}\langle B^{-2}\rangle\right)\langle B^2\{u_{ip\mathbf{k}_\perp}(0)+u_{ip\mathbf{k}_\perp}^{(s)}(t)\}/B_p\rangle - K_i^2\frac{T_i}{m_i}\langle\{u_{ip\mathbf{k}_\perp}(0)+u_{ip\mathbf{k}_\perp}^{(s)}(t)\}/B_p\rangle\right]. \tag{23}$$

Also, the parallel component $u_{i\parallel\mathbf{k}_\perp}(t)$ is immediately derived from substituting Eqs. (22) and (23) and into Eq. (A7) while the toroidal component $u_{it\mathbf{k}_\perp}(t)$ is obtained by substituting Eqs. (22) and (23) into Eq. (A2).

We see from Eq. (23) that the poloidal flow component depends on the initial condition only through the initial poloidal flow. This dependence is affected by the poloidal-angle dependence of the initial poloidal flow. For example, let us assume $B^2[u_{ip\mathbf{k}_\perp}(0)/B_p]$ to be constant on the flux surface. As shown from Eq. (A3), this condition is satisfied when $Bu_{i\parallel\mathbf{k}_\perp}(0)$ is constant on the flux surface, the special case of which is give by no initial parallel flow, $u_{i\parallel\mathbf{k}_\perp}(0)=0$. Then, for the case of no turbulence source, Eq. (23) gives

$$\frac{u_{ip\mathbf{k}_\perp}(t)/B_p}{\langle u_{ip\mathbf{k}_\perp}(0)/B_p\rangle} = \frac{\beta_1}{\langle B^{-2}\rangle}\frac{n_0\langle k_\perp^2 a_i^2\rangle}{\mathcal{D}_{\rm ITG}}. \tag{24}$$

As another example, we consider the initial flow to be incompressible. In this case, the initial poloidal flow satisfies the condition $u_{ip\mathbf{k}_\perp}(0)/B_p=\langle u_{ip\mathbf{k}_\perp}(0)/B_p\rangle$ [see Eq. (A12)] and Eq. (23) leads to

$$\frac{u_{ip\mathbf{k}_\perp}(t)/B_p}{\langle u_{ip\mathbf{k}_\perp}(0)/B_p\rangle} = \frac{n_0}{\mathcal{D}_{\rm ITG}}\beta_1\langle k_\perp^2 a_i^2 B^2/R^2\rangle\langle R^2\rangle(1+2\hat{q}^2), \tag{25}$$

where $\hat{q}$ is defined by Eq. (A6). The ratio in Eq. (25) gives a significantly higher value than that in Eq. (24). This interesting result is not clearly pointed out in the original work by Rosenbluth and Hinton although it can be understood by noting that the incompressible flow does not contain such a GAM part that should be Landau-damped in the long-time evolution. Especially, when there is no initial poloidal flow $u_{ip\mathbf{k}_\perp}(0)=0$, which means the finite initial parallel flow given from Eq. (A3) as $u_{i\parallel\mathbf{k}_\perp}(0)=-(B_t/B_p)u_{i\perp\mathbf{k}_\perp}(0)=-ick_\perp(B_t/B_p)\phi_{\mathbf{k}_\perp}(0)/B$, Eqs. (22) and (23) show that, for the case with no turbulence source, $\phi_{\mathbf{k}_\perp}(t)=\phi_{\mathbf{k}_\perp}(0)$ and $u_{ip\mathbf{k}_\perp}(t)=0$ so that the zonal flow remains in the toroidal direction and has the same magnitude all the time. This is a natural result in axisymmetric systems and we can also confirm from using Eq. (16), and $u_{i\parallel\mathbf{k}_\perp}(t)=-ick_\perp(B_t/B_p)\phi_{\mathbf{k}_\perp}(t)/B$ that the shifted Maxwellian distribution function corresponding to the toroidal rotation becomes a good approximate stationary solution of the linearized gyrokinetic-Poisson system of equations for $k_\perp a_i \ll 1$.

For a large-aspect-ratio toroidal flux surface which has a major radius R_0 and a circular cross section with a radius r, the magnetic-field strength is written as $B=B_0(1-\epsilon\cos\theta)$ and we have

$$\beta_1 = B_0^{-2}(1-C\epsilon^{3/2}). \tag{26}$$

Here, the dimensionless coefficient C is evaluated as

$$C \equiv 6\sqrt{2}\left\{\frac{4}{9\pi} + \int_0^1 \frac{d\kappa}{\kappa^4}\left[\frac{2}{\pi}E(\kappa) - \frac{\pi}{2K(\kappa)}\right]\right\}$$
$$\equiv \sqrt{2}\left\{\frac{1}{2} + 6\int_0^1\frac{d\kappa}{\kappa^4}\left[1-\frac{\kappa^2}{4}-\frac{\pi}{2K(\kappa)}\right]\right\} \simeq 1.6, \tag{27}$$

where $K(\kappa)$ and $E(\kappa)$ are the complete elliptic integrals of the first and second kinds, respectively. Then, Eq. (20) reduces to

$$\mathcal{D}_{\rm ITG} = n_0\langle k_\perp^2 a_i^2\rangle(1+1.6q^2/\epsilon^{1/2}), \tag{28}$$

where $\epsilon \equiv r/R_0$ is the inverse aspect ratio, $q\equiv \epsilon B_t/B_p$ is the safety factor, and $K_i=k_r qB_0/(\epsilon\Omega_i)$ is used. We see from Eqs. (22) and (24) that, if no turbulence source exists, the well-known Rosenbluth-Hinton formula[7] is obtained for the case of no initial parallel flow as

$$\frac{\phi_{\mathbf{k}}(t)}{\phi_{\mathbf{k}}(0)} = \frac{u_{ip\mathbf{k}_\perp}(t)/B_p}{\langle u_{ip\mathbf{k}_\perp}(0)/B_p\rangle} = \frac{1}{1+1.6q^2/\epsilon^{1/2}}, \tag{29}$$

which is often used for benchmark tests of gyrokinetic simulation codes.[10,11] Also, it is shown from Eqs. (24) and (25) that, when there is a finite parallel flow initially, the ratio of the poloidal flow to its initial value is given for the case of $Bu_{i\|\mathbf{k}_\perp}(0)=\langle Bu_{i\|\mathbf{k}_\perp}(0)\rangle$ by

$$\frac{u_{ip\mathbf{k}_\perp}(t)/B_p}{\langle u_{ip\mathbf{k}_\perp}(0)/B_p\rangle} = \frac{1}{1+1.6q^2/\epsilon^{1/2}}, \tag{30}$$

while it is written under the condition of the incompressible initial flow, $u_{ip\mathbf{k}_\perp}(0)/B_p=\langle u_{ip\mathbf{k}_\perp}(0)/B_p\rangle$, as

$$\frac{u_{ip\mathbf{k}_\perp}(t)/B_p}{\langle u_{ip\mathbf{k}_\perp}(0)/B_p\rangle} = \frac{1+2q^2}{1+1.6q^2/\epsilon^{1/2}}. \tag{31}$$

We should note that the efficiency of the zonal-flow generation by the ITG turbulence should be measured not by Eq. (29) but, for example, by

$$\frac{e\phi_{\mathbf{k}_\perp}(t)/T_i}{\langle \delta n^{(s)}_{i\mathbf{k}_\perp}(t)\rangle/n_0} = \frac{e\phi_{\mathbf{k}_\perp}(t)/T_i}{\left\langle \int d^3v F_0 R_{i\mathbf{k}_\perp}(t)\right\rangle/n_0} = \frac{n_0}{\mathcal{D}_{\rm ITG}} = \frac{1}{\langle k_\perp^2 a_i^2\rangle(1+1.6q^2/\epsilon^{1/2})}, \tag{32}$$

which is obtained from Eq. (22) by neglecting the initial-value and parallel-flow terms. Equation (32) represents the ratio of the zonal-flow potential to the time- and velocity-integrated nonlinear source term and it is larger than the ratio to the initial potential value in Eq. (29) by the factor of $1/\langle k_\perp^2 a_i^2\rangle$.

2. Residual zonal flows in ETG turbulence

Now, we consider the wave-number region $1/a_i \ll k_\perp < 1/a_e$ where $a_e \equiv (T_e/m_e)^{1/2}/|\Omega_e|$ in order to investigate collisionless residual zonal flows in the ETG turbulence. ETG-mode-driven zonal flows were analytically treated by Kim *et al.*[14] who also studied collisional effects on them. Here, in Eq. (3), we put $\Gamma_0(b_i)\simeq 0$, $1-\Gamma_0(b_e)\simeq b_e \equiv k_\perp^2 a_e^2$, and neglect $\int d^3v J_0 \delta f^{(g)}_{i\mathbf{k}_\perp}$ because $k_\perp a_i \gg 1$. Thus, the perturbed ion density is given by the Boltzmann relation $\delta n_{i\mathbf{k}_\perp}/n_0 = -e\phi_{\mathbf{k}_\perp}/T_i$. Then, substituting Eq. (15) for electrons into Eq. (3) and taking its flux-surface average, we obtain

$$\frac{e\phi_{\mathbf{k}_\perp}(t)}{T_e} = \frac{-1}{\mathcal{D}_{\rm ETG}}\left\langle \int d^3v \left\{ 1 + iK_e[(v_\|/B) - \overline{(v_\|/B)}] + K_e^2\left[(v_\|/B)\overline{(v_\|/B)} - \frac{1}{2}(v_\|/B)^2 - \frac{1}{2}\overline{(v_\|/B)^2}\right] - \frac{1}{4}k_\perp^2\rho_e^2\right\}[\overline{\delta f^{(g)}_{e\mathbf{k}_\perp}}(0) + F_{e0}\overline{R_{e\mathbf{k}_\perp}}(t)]\right\rangle, \tag{33}$$

where

$$\begin{aligned}\mathcal{D}_{\rm ETG} &\equiv n_0\left[\frac{T_e}{T_i} + \langle k_\perp^2(a_e^2+\lambda_{\rm De}^2)\rangle\right] + \left\langle \int d^3v F_{e0}K_e^2[\overline{(v_\|/B)^2} - (\overline{v_\|/B})^2]\right\rangle \\ &= n_0\left[\frac{T_e}{T_i} + \langle k_\perp^2(a_e^2+\lambda_{\rm De}^2)\rangle + K_e^2\frac{T_e}{m_e}(\langle B^{-2}\rangle - \beta_1)\right] \\ &= n_0\left[\frac{T_e}{T_i} + \langle k_\perp^2 a_{ep}^2(1-\beta_1 B_t^2)\rangle + \langle k_\perp^2\lambda_{\rm De}^2\rangle\right].\end{aligned} \tag{34}$$

Equations (33) and (34) contain terms up to $\mathcal{O}(k_\perp^2 a_e^2)$ although, if keeping only terms of the leading order in $k_\perp a_e$, they give $\delta n_{e\mathbf{k}_\perp}(t)=\delta n_{i\mathbf{k}_\perp}(t)=-n_0 e\phi_{\mathbf{k}_\perp}(t)/T_i \simeq \int d^3v[\overline{\delta f^{(g)}_{e\mathbf{k}_\perp}}(0)+F_{e0}\overline{R_{e\mathbf{k}_\perp}}(t)]$, from which Eq. (A9) is derived by noting $\phi_{\mathbf{k}_\perp}=\langle\phi_{\mathbf{k}_\perp}\rangle$. Then, on the leading order in $k_\perp a_e$, the perpendicular electron flow is written from Eq. (A4) as $u_{e\perp\mathbf{k}_\perp}=ick_\perp\phi_{e*\mathbf{k}_\perp}/B$ with

$$\begin{aligned}\phi_{e*\mathbf{k}_\perp}(t) &\equiv \phi_{\mathbf{k}_\perp}(t) - (T_e/e)\langle\delta n_{e\mathbf{k}_\perp}(t)\rangle/n_0 \\ &= (1+T_e/T_i)\phi_{\mathbf{k}_\perp}(t).\end{aligned} \tag{35}$$

Using Eqs. (A14), (A15), and (3) for $t=0$, Eq. (33) is rewritten up to $\mathcal{O}(k_\perp a_e^2)$ as

$$\begin{aligned}\frac{e\phi_{\mathbf{k}_\perp}(t)}{T_e} &= \frac{n_0}{\mathcal{D}'_{\rm ETG}}\left\{\left[\frac{T_e}{T_i}+\langle k_\perp^2(a_e^2+\lambda_{\rm De}^2)\rangle\right]\frac{e\phi_{\mathbf{k}_\perp}(0)}{T_e} - \frac{\langle e^{-b_e/2}\delta n^{(s)}_{e\mathbf{k}_\perp}(t)\rangle}{n_0} - iK_e\{\langle[u_{e\|\mathbf{k}_\perp}(0)+u^{(s)}_{e\|\mathbf{k}_\perp}(t)]/B\rangle - \beta_1\langle[u_{e\|\mathbf{k}_\perp}(0)+u^{(s)}_{e\|\mathbf{k}_\perp}(t)]B\rangle\}\right\} \\ &= \frac{e\phi_{\mathbf{k}_\perp}(0)}{T_e} - i\frac{n_0 K_e}{\mathcal{D}'_{\rm ETG}}\{\langle[u_{ep\mathbf{k}_\perp}(0)+u^{(s)}_{ep\mathbf{k}_\perp}(t)]/B_p\rangle - \beta_1\langle B^2[u_{ep\mathbf{k}_\perp}(0)+u^{(s)}_{ep\mathbf{k}_\perp}(t)]/B_p\rangle\},\end{aligned} \tag{36}$$

where the modified shielding function $\mathcal{D}'_{\rm ETG}$ is given by

$$\mathcal{D}'_{\rm ETG} \equiv \mathcal{D}_{\rm ETG}\{1 + K_e^2(T_e/m_e)(\langle B^{-2}\rangle - \beta_1)\}$$
$$\simeq n_0\left[\frac{T_e}{T_i} + \langle k_\perp^2(a_e^2+\lambda_{\rm De}^2)\rangle + K_e^2\frac{T_e}{m_e}\left(1+\frac{T_e}{T_i}\right)(\langle B^{-2}\rangle - \beta_1)\right] \quad (37)$$

and $u^{(s)}_{ep\mathbf{k}_\perp}(t)$ is defined by $u^{(s)}_{ep\mathbf{k}_\perp}(t)=[B_p u^{(s)}_{e\|\mathbf{k}_\perp}(t)+B_t u^{(s)}_{e\perp\mathbf{k}_\perp}(t)]/B$. Here, the source terms similar to those in Eq. (18) are defined by

$$u^{(s)}_{e\|\mathbf{k}_\perp}(t) \equiv \frac{1}{n_0}\int d^3v F_{e0}R_{e\mathbf{k}_\perp}(t)v_\|,$$

$$u^{(s)}_{e\perp\mathbf{k}_\perp}(t) \equiv \frac{ick_\perp\phi^{(s)}_{\mathbf{k}_\perp}(t)}{B}\left(1+\frac{T_e}{T_i}\right), \quad (38)$$
$$\langle e^{-b_e/2}\delta n^{(s)}_{e\mathbf{k}_\perp}(t)\rangle \equiv -n_0\frac{e\phi^{(s)}_{\mathbf{k}_\perp}(t)}{T_e}\left[\frac{T_e}{T_i}+\langle k_\perp^2(a_e^2+\lambda_{\rm De}^2)\rangle\right] \equiv \left\langle \int d^3v J_0(k_\perp\rho_e)F_{e0}R_{e\mathbf{k}_\perp}(t)\right\rangle.$$

Dependence of the perpendicular long-time zonal-flow component $u_{e\perp\mathbf{k}_\perp}(t)$ on the initial condition and the turbulence source is given by $u_{e\perp\mathbf{k}_\perp}(t)=ick_\perp\phi_{e*\mathbf{k}_\perp}(t)/B=ick_\perp(1+T_e/T_i)\phi_{\mathbf{k}_\perp}(t)/B$ with Eq. (36). Substituting Eq. (36) into Eq. (A8) and using Eq. (A10) gives the electron poloidal zonal-flow component as

$$u_{ep\mathbf{k}_\perp}(t)/B_p = \frac{n_0\beta_1}{\mathcal{D}'_{\rm ETG}}\Bigg(-iK_e\frac{T_e}{m_e}\left(1+\frac{T_e}{T_i}\right)\left\{\left[\frac{T_e}{T_i}+\langle k_\perp^2(a_e^2+\lambda_{\rm De}^2)\rangle\right]\frac{e\phi_{\mathbf{k}_\perp}(0)}{T_i} - \frac{\langle e^{-b_e/2}\delta n^{(s)}_{e\mathbf{k}_\perp}(t)\rangle}{n_0}\right\}$$
$$+\left[\frac{T_e}{T_i}+\langle k_\perp^2(a_e^2+\lambda_{\rm De}^2)\rangle + K_e^2\frac{T_e}{m_e}\left(1+\frac{T_e}{T_i}\right)\langle B^{-2}\rangle\right]$$
$$\times\langle[u_{e\|\mathbf{k}_\perp}(0)+u^{(s)}_{e\|\mathbf{k}_\perp}(t)]B\rangle - K_e^2\frac{T_e}{m_e}\left(1+\frac{T_e}{T_i}\right)\langle[u_{e\|\mathbf{k}_\perp}(0)+u^{(s)}_{e\|\mathbf{k}_\perp}(t)]/B\rangle\Bigg)$$
$$= \frac{n_0\beta_1}{\mathcal{D}'_{\rm ETG}}\Bigg\{\left[\frac{T_e}{T_i}+\langle k_\perp^2(a_e^2+\lambda_{\rm De}^2)\rangle + K_e^2\frac{T_e}{m_e}\left(1+\frac{T_e}{T_i}\right)\langle B^{-2}\rangle\right]\langle B^2[u_{ep\mathbf{k}_\perp}(0)+u^{(s)}_{ep\mathbf{k}_\perp}(t)]/B_p\rangle$$
$$- K_e^2\frac{T_e}{m_e}\left(1+\frac{T_e}{T_i}\right)\langle[u_{ep\mathbf{k}_\perp}(0)+u^{(s)}_{ep\mathbf{k}_\perp}(t)]/B_p\rangle\Bigg\}. \quad (39)$$

The parallel component $u_{e\|\mathbf{k}_\perp}(t)$ is immediately derived from substituting Eqs. (36) and (39) into Eq. (A7) while the toroidal component $u_{et\mathbf{k}_\perp}(t)$ is obtained by substituting Eqs. (36) and (39) into Eq. (A2).

In the same way as shown for the ion poloidal flow in Eq. (23), Eq. (39) shows that the electron poloidal flow depends on the initial condition only through its initial value and that this dependence is affected by the poloidal-angle dependence of the initial poloidal flow. When $Bu_{e\|\mathbf{k}_\perp}(0)$ is constant on the flux surface, $B^2(u_{ep\mathbf{k}_\perp}(0)/B_p)$ is also constant on the flux surface and Eq. (39) for the case of no turbulence source gives

$$\frac{u_{ep\mathbf{k}_\perp}(t)/B_p}{\langle u_{ep\mathbf{k}_\perp}(0)/B_p\rangle} = \frac{n_0\beta_1}{\mathcal{D}'_{\rm ETG}\langle B^{-2}\rangle}\left\{\frac{T_e}{T_i}+\langle k_\perp^2(a_e^2+\lambda_{\rm De}^2)\rangle\right\}. \quad (40)$$

In another case, where the initial electron flow is incompressible, we have $u_{ep\mathbf{k}_\perp}(0)/B_p=\langle u_{ep\mathbf{k}_\perp}(0)/B_p\rangle$ and Eq. (39) yields

$$\frac{u_{ep\mathbf{k}_\perp}(t)/B_p}{\langle u_{ep\mathbf{k}_\perp}(0)/B_p\rangle} = \frac{n_0\beta_1\langle B^2\rangle}{\mathcal{D}'_{\rm ETG}}\left[\frac{T_e}{T_i}(1-\langle k_\perp^2 a_e^2\rangle)+\langle k_\perp^2\lambda_{\rm De}^2\rangle + \langle k_\perp^2 a_e^2 B^2/R^2\rangle\frac{\langle R^2\rangle}{\langle B^2\rangle}\left(1+\frac{T_e}{T_i}\right)(1+2\hat{q}^2)\right]. \quad (41)$$

We also find from Eqs. (36) and (39) that, if the initial electron poloidal flow and the source terms both vanish, the electrostatic potential and the zonal-flow components in all directions remain unchanged.

For a large-aspect-ratio toroidal flux surface, we follow the same procedure as adopted in Eqs. (28)–(32) and rewrite Eq. (37) by

$$\mathcal{D}'_{\rm ETG} = n_0\left\{\frac{T_e}{T_i}+\langle k_\perp^2\lambda_{\rm De}^2\rangle + \langle k_\perp^2 a_e^2\rangle \times\left[1+1.6\left(1+\frac{T_e}{T_i}\right)\frac{q^2}{\epsilon^{1/2}}\right]\right\}. \quad (42)$$

In the case, where neither the initial parallel flow nor the turbulence source exists, we find from Eqs. (36) and (39) that

$$\frac{\phi_{\mathbf{k}_\perp}(t)}{\phi_{\mathbf{k}_\perp}(0)} = \frac{u_{ep\mathbf{k}_\perp}(t)/B_p}{\langle u_{ep\mathbf{k}_\perp}(0)/B_p\rangle} = \frac{T_e/T_i + \langle k_\perp^2(a_e^2+\lambda_{\rm De}^2)\rangle}{T_e/T_i + \langle k_\perp^2 a_e^2\rangle[1+1.6(1+T_e/T_i)q^2/\epsilon^{1/2}] + \langle k_\perp^2\lambda_{\rm De}^2\rangle}. \tag{43}$$

The denominator on the right-hand side of Eq. (43) contains a term $\propto\langle k_\perp^2 a_e^2\rangle(T_e/T_i)q^2/\epsilon^{1/2}$ that is missed by Kim *et al.*[14] This term comes from the last group of terms proportional to $K^2\delta f_{\mathbf{k}_\perp}^{(g)}(0)$ in Eq. (15) which are neglected in Ref. 14 but necessary to keep for the accuracy of $\mathcal{O}(k_\perp^2 a_e^2)$. Using Eqs. (40) and (41), the ratio of the electron poloidal flow to its initial value is written as

$$\frac{u_{ep\mathbf{k}_\perp}(t)/B_p}{\langle u_{ep\mathbf{k}_\perp}(0)/B_p\rangle} = \frac{T_e/T_i + \langle k_\perp^2(a_e^2+\lambda_{\rm De}^2)\rangle}{T_e/T_i + \langle k_\perp^2 a_e^2\rangle[1+1.6(1+T_e/T_i)q^2/\epsilon^{1/2}] + \langle k_\perp^2\lambda_{\rm De}^2\rangle} \tag{44}$$

for $Bu_{e\parallel\mathbf{k}_\perp}(0)=\langle Bu_{e\parallel\mathbf{k}_\perp}(0)\rangle$, and

$$\frac{u_{ep\mathbf{k}_\perp}(t)/B_p}{\langle u_{ep\mathbf{k}_\perp}(0)/B_p\rangle} = \frac{(T_e/T_i)[1+2\langle k_\perp^2 a_e^2\rangle q^2] + \langle k_\perp^2 a_e^2\rangle(1+2q^2) + \langle k_\perp^2\lambda_{\rm De}^2\rangle}{T_e/T_i + \langle k_\perp^2 a_e^2\rangle[1+1.6(1+T_e/T_i)q^2/\epsilon^{1/2}] + \langle k_\perp^2\lambda_{\rm De}^2\rangle} \tag{45}$$

for the case of the incompressible initial flow, $u_{ep\mathbf{k}_\perp}(0)/B_p =\langle u_{ep\mathbf{k}_\perp}(0)/B_p\rangle$.

Parallel to Eq. (32), the efficiency of the zonal-flow generation by the ETG turbulence can be characterized by

$$\begin{aligned}\frac{e\phi_{\mathbf{k}_\perp}(t)/T_e}{\langle\delta n_{e\mathbf{k}_\perp}^{(s)}(t)\rangle/n_0} &= \frac{e\phi_{\mathbf{k}_\perp}(t)/T_e}{\left\langle\int d^3v F_{e0}R_{e\mathbf{k}_\perp}(t)\right\rangle/n_0} \\ &= -\frac{n_0\langle e^{-b_e/2}\rangle}{\mathcal{D}'_{\rm ETG}} \\ &= -\left\{\frac{T_e}{T_i} + \langle k_\perp^2\lambda_{\rm De}^2\rangle + \langle k_\perp^2 a_e^2\rangle\left[\left(1+\frac{T_e}{2T_i}\right)\right.\right. \\ &\quad \left.\left. + \left(1+\frac{T_e}{T_i}\right)\left(1+1.6\frac{q^2}{\epsilon^{1/2}}\right)\right]\right\}^{-1},\end{aligned} \tag{46}$$

which is obtained from Eq. (36) by neglecting the initial-value and parallel-flow terms. A comparison between Eqs. (32) and (46) shows higher zonal-flow generation by the ITG turbulence than by the ETG turbulence because $\mathcal{D}_{\rm ITG}$ is proportional to the factor $\langle k_\perp^2 a_i^2\rangle$.

III. KINETIC-FLUID MODEL OF ZONAL FLOWS

In this section, the kinetic-fluid equations to describe zonal flows are presented, which include novel closure relations for parallel heat fluxes. It is analytically found that the kinetic-fluid model yields the same residual zonal-flow levels as predicted by the gyrokinetic model for both cases of the ITG and ETG turbulence.

A. Kinetic-fluid equations

Now let us take the velocity moments of Eq. (1) to obtain the equations which govern time evolution of the fluid variables defined by

$$\begin{aligned}&[\delta n_{\mathbf{k}_\perp}^{(g)}, n_0 u_{\parallel\mathbf{k}_\perp}, \delta p_{\parallel\mathbf{k}_\perp}, \delta p_{\perp\mathbf{k}_\perp}] \\ &\quad = \int d^3v\,\delta f_{\mathbf{k}_\perp}^{(g)}\left[1, v_\parallel, mv_\parallel^2, \frac{1}{2}mv_\perp^2\right].\end{aligned} \tag{47}$$

Consequently, we obtain the perturbed gyrocenter density equation,

$$\begin{aligned}&\frac{\partial\delta n_{\mathbf{k}_\perp}^{(g)}}{\partial t} + \mathbf{B}\cdot\nabla\left(\frac{n_0 u_{\parallel\mathbf{k}_\perp}}{B}\right) \\ &\quad = -i\frac{c}{eB^2}\mathbf{k}_\perp\cdot(\mathbf{b}\times\nabla B)[\delta p_{\parallel\mathbf{k}_\perp} + \delta p_{\perp\mathbf{k}_\perp} \\ &\qquad + n_0 e\phi_{\mathbf{k}_\perp}e^{-b/2}(2-b/2)] + \mathcal{N}_{0\mathbf{k}_\perp},\end{aligned} \tag{48}$$

the parallel momentum balance equation,

$$\begin{aligned}&mn_0\frac{\partial u_{\parallel\mathbf{k}_\perp}}{\partial t} + \mathbf{B}\cdot\nabla\left(\frac{\delta p_{\parallel\mathbf{k}_\perp}}{B}\right) + \frac{\delta p_{\perp\mathbf{k}_\perp}}{B}\mathbf{b}\cdot\nabla B \\ &\quad = -i\frac{mc}{eB^2}\mathbf{k}_\perp\cdot(\mathbf{b}\times\nabla B)(q_{\parallel\mathbf{k}_\perp} + q_{\perp\mathbf{k}_\perp} + 4p_0 u_{\parallel\mathbf{k}_\perp}) \\ &\qquad - n_0 e\mathbf{b}\cdot\nabla(\phi_{\mathbf{k}_\perp}e^{-b/2}) + \frac{n_0 eb}{2B}\phi_{\mathbf{k}_\perp}e^{-b/2}\mathbf{b}\cdot\nabla B \\ &\qquad + \mathcal{N}_{1\mathbf{k}_\perp},\end{aligned} \tag{49}$$

the perturbed parallel pressure equation,

$$\begin{aligned}&\frac{\partial\delta p_{\parallel\mathbf{k}_\perp}}{\partial t} + \mathbf{B}\cdot\nabla[(q_{\parallel\mathbf{k}_\perp} + 3p_0 u_{\parallel\mathbf{k}_\perp})/B] \\ &\quad + \frac{2}{B}(q_{\perp\mathbf{k}_\perp} + p_0 u_{\parallel\mathbf{k}_\perp})\mathbf{b}\cdot\nabla B \\ &\quad = -i\frac{c}{eB^2}\mathbf{k}_\perp\cdot(\mathbf{b}\times\nabla B)[m(\delta r_{\parallel,\parallel\mathbf{k}_\perp} + \delta r_{\parallel,\perp\mathbf{k}_\perp}) \\ &\qquad + p_0 e\phi_{\mathbf{k}_\perp}e^{-b/2}(4-b/2)] + \mathcal{N}_{2\parallel\mathbf{k}_\perp},\end{aligned} \tag{50}$$

and the perturbed perpendicular pressure equation,

$$\frac{\partial \delta p_{\perp \mathbf{k}_\perp}}{\partial t} + \mathbf{B}\cdot\nabla[(q_{\perp \mathbf{k}_\perp} + p_0 u_{\parallel \mathbf{k}_\perp})/B] - \frac{1}{B}(q_{\perp \mathbf{k}_\perp} + p_0 u_{\parallel \mathbf{k}_\perp})\mathbf{b}\cdot\nabla B = -i\frac{c}{eB^2}\mathbf{k}_\perp\cdot(\mathbf{b}\times\nabla B)[m(\delta r_{\parallel,\perp \mathbf{k}_\perp} + \delta r_{\perp,\perp \mathbf{k}_\perp}) + p_0 e\phi_{\mathbf{k}_\perp} e^{-b/2}(3-3b/2+b^2/8)] + \mathcal{N}_{2\perp \mathbf{k}_\perp}, \tag{51}$$

where $\mathcal{N}_{0\mathbf{k}_\perp}$, $\mathcal{N}_{1\mathbf{k}_\perp}$, $\mathcal{N}_{2\parallel \mathbf{k}_\perp}$, and $\mathcal{N}_{2\perp \mathbf{k}_\perp}$ are the nonlinear source terms defined by

$$[\mathcal{N}_{0\mathbf{k}_\perp}, \mathcal{N}_{1\mathbf{k}_\perp}, \mathcal{N}_{2\parallel \mathbf{k}_\perp}, \mathcal{N}_{2\perp \mathbf{k}_\perp}] = \int d^3v F_0 S_{\mathbf{k}_\perp}\left[1, mv_\parallel, mv_\parallel^2, \frac{1}{2}mv_\perp^2\right]. \tag{52}$$

We also define the perturbed parallel and perpendicular temperatures $(\delta T_{\parallel \mathbf{k}_\parallel}, \delta T_{\perp \mathbf{k}_\perp})$ by the following relations:

$$\delta p_{\parallel \mathbf{k}_\perp} = n_0 \delta T_{\parallel \mathbf{k}_\perp} + T\delta n^{(g)}_{\mathbf{k}_\perp}, \quad \delta p_{\perp \mathbf{k}_\perp} = n_0 \delta T_{\perp \mathbf{k}_\perp} + T\delta n^{(g)}_{\mathbf{k}_\perp}. \tag{53}$$

The right-hand sides of Eqs. (49)–(51) contain the third-order fluid variables (or parallel heat fluxes),

$$[q_{\parallel \mathbf{k}_\perp}, q_{\perp \mathbf{k}_\perp}] = \int d^3v\, \delta f^{(g)}_{\mathbf{k}_\perp} v_\parallel \left[(mv_\parallel^2 - 3T), \left(\frac{1}{2}mv_\perp^2 - T\right)\right], \tag{54}$$

and the fourth-order fluid variables,

$$[\delta r_{\parallel,\parallel \mathbf{k}_\perp}, \delta r_{\parallel,\perp \mathbf{k}_\perp}, \delta r_{\perp,\perp \mathbf{k}_\perp}] = \int d^3v\, \delta f^{(g)}_{\mathbf{k}_\perp} m\left[v_\parallel^4, \frac{1}{2}v_\parallel^2 v_\perp^2, \frac{1}{4}v_\perp^4\right]. \tag{55}$$

In order to construct a closed system of kinetic-fluid equations, we need to use Poisson's equation, Eq. (3) as well as devise so-called *closure* relations, which express the higher-order fluid variables in Eqs. (54) and (55) in terms of the lower-order variables in Eq. (47).

B. Closure model

We write the parallel heat fluxes as the sum of long- and short-time evolution parts,

$$q_{\parallel \mathbf{k}_\perp} = q^{(l)}_{\parallel \mathbf{k}_\perp} + q^{(s)}_{\parallel \mathbf{k}_\perp}, \quad q_{\perp \mathbf{k}_\perp} = q^{(l)}_{\perp \mathbf{k}_\perp} + q^{(s)}_{\perp \mathbf{k}_\perp}. \tag{56}$$

Evaluating the parallel heat fluxes by using Eq. (15), which describes the long-time behavior of the perturbed gyrocenter distribution function, and making use of Eqs. (A7)–(A10), we obtain

$$q^{(l)}_{\parallel \mathbf{k}_\perp} = -2q^{(l)}_{\perp \mathbf{k}_\perp} = 2p_0 U_{\mathbf{k}_\perp}\left(B - \frac{\beta_2}{\beta_1}B^2\right), \tag{57}$$

where

$$U_{\mathbf{k}_\perp} \equiv \beta_1(\beta_1 - \langle B^{-2}\rangle)^{-1}\left(\left\langle \frac{u_{\parallel \mathbf{k}_\perp}}{B}\right\rangle - \langle B^{-2}\rangle\langle B u_{\parallel \mathbf{k}_\perp}(t=0)\rangle - \frac{\langle B^{-2}\rangle}{\beta_1 n_0}\left\langle \int d^3v F_0 R_{\mathbf{k}_\perp}(t)\overline{\left(\frac{v_\parallel}{B}\right)}\right\rangle\right), \tag{58}$$

$$\beta_2 \equiv \frac{15}{4}\int_0^{1/B_M} \frac{\lambda d\lambda}{\langle B/(1-\lambda B)^{1/2}\rangle}, \tag{59}$$

and β_1 is defined by Eq. (21).

In order to consider the short-time phenomena such as the GAM oscillations, we neglect trapped-particle effects and the perpendicular drift term in the left-hand side of Eq. (1). Then, we find from Eq. (1) that the perturbed gyrocenter distribution function is given in the form of

$$\delta f^{(g)}_{m\mathbf{k}_\perp} = F_0 \frac{c_{0\mathbf{k}_\perp} v_\parallel + c_{1\mathbf{k}_\perp} v_\parallel^2 + c_{2\mathbf{k}_\perp} v_\perp^2}{\omega - m(v_\parallel / R_0 q)} \tag{60}$$

where the coefficients $c_{j\mathbf{k}_\perp}$ $(j=0,1,2)$ are independent of the velocity variables and the integer m represents the mode number in the Fourier series of the arbitrary periodic function of θ as given by $g(\theta)=\Sigma_m g_m e^{im\theta}$. In deriving Eq. (60), $\partial/\partial t = -i\omega$ and $\mathbf{b}\cdot\nabla e^{im\theta} = ime^{im\theta}/(R_0 q)$ with the major radius R_0 are used and the nonlinear source term is neglected compared with the time-derivative term in Eq. (1) for the short-time evolution. In fact, for the case of the GAM oscillations of ion zonal flows, we find that $\omega \sim v_{ti}/R_0 \gg k_r v_{dri}$ and that trapped ions are nonresonant and noninfluential in the GAM dispersion relation. Then, using Eq. (60) and taking the adiabatic approximation $R_0 q\omega/(mv_t) \to 0$ lead to the parallel heat fluxes in the same dissipative form as in Hammett and Perkins,[17]

$$q^{(s)}_{\parallel m\mathbf{k}_\perp} = -2\left(\frac{2}{\pi}\right)^{1/2} i\frac{m}{|m|} n_0 v_t \delta T_{\parallel m\mathbf{k}_\perp}, \quad q^{(s)}_{\perp m\mathbf{k}_\perp} = -\left(\frac{2}{\pi}\right)^{1/2} i\frac{m}{|m|} n_0 v_t \delta T_{\perp m\mathbf{k}_\perp}, \tag{61}$$

where $v_t \equiv (T/m)^{1/2}$. If we use the GAM frequency as ω for the ion zonal-flow case and take $m=1$, we have $R_0 q|\omega|/v_t > 1$ so that the fluid-approximation limit $R_0 q|\omega|/v_t \to +\infty$ may seem better than the adiabatic approximation. However, it should be noted that collisionless damping of the GAM is never derived from taking the fluid-approximation limit while the adiabatic approximation gives rise to the reasonable GAM damping rate.

As done in deriving Eq. (60), the short-time-evolution part of $\delta f^{(g)}_{\mathbf{k}_\perp}$ is evaluated by balancing the linear terms in Eq. (1) and is used to estimate the magnitudes of the fourth-order variables $(\delta r_{\parallel,\parallel \mathbf{k}_\perp}, \delta r_{\parallel,\perp \mathbf{k}_\perp}, \delta r_{\perp,\perp \mathbf{k}_\perp})$. Then, we see that, for $R_0 q|\omega|/v_t > 1$ and $k_\perp^{-1} > a(\equiv \sqrt{T/m}/\Omega)$, $\delta r_{\mathbf{k}_\perp}$ terms are regarded as negligible compared with the $\phi_{\mathbf{k}_\perp}$ terms in Eqs. (50) and (51). On the other hand, for the long-time evolution, we use Eqs. (15), (A14), and (A15), with terms up to $\mathcal{O}(K)$ retained and find that only the even parts of Eqs. (A14) and

(A15), which take the Maxwellian form, contribute to $(\delta r_{\parallel\parallel\mathbf{k}_\perp}, \delta r_{\parallel\perp\mathbf{k}_\perp}, \delta r_{\perp\perp\mathbf{k}_\perp})$. Thus, we finally obtain

$$[\delta r_{\parallel\parallel\mathbf{k}_\perp}, \delta r_{\parallel\perp\mathbf{k}_\perp}, \delta r_{\perp\perp\mathbf{k}_\perp}] = v_t^2 T \delta n_{\mathbf{k}_\perp}^{(g)}[3,1,2]. \tag{62}$$

Here, it should be noted that the collisionless zonal-flow damping are modeled not by these closure relations for the fourth-order variables but by those for the third-order variables in Eq. (61).

C. Balance equations

A balance equation corresponding to Eq. (10) is derived from Eqs. (48)–(50) as

$$\frac{\partial}{\partial t}\left\langle \delta n_{\mathbf{k}_\perp}^{(g)} + i\left(\frac{K}{B}\right) n_0 u_{\parallel\mathbf{k}_\perp} - \left(\frac{K}{B}\right)^2 \frac{\delta p_{\parallel\mathbf{k}_\perp}}{2m}\right\rangle = \left\langle \mathcal{N}_{0\mathbf{k}_\perp} + \frac{i}{m}\left(\frac{K}{B}\right)\mathcal{N}_{1\mathbf{k}_\perp} - \frac{1}{2m}\left(\frac{K}{B}\right)^2 \mathcal{N}_{2\parallel\mathbf{k}_\perp}\right\rangle, \tag{63}$$

where small terms of $\mathcal{O}(K^3)$ are neglected. Here, we consider the long-time evolution of the fluid variables, for which $q_{\parallel\mathbf{k}_\perp}^{(s)}$, $q_{\perp\mathbf{k}_\perp}^{(s)}$, $\tilde{\phi}_{\mathbf{k}_\perp}$, and $\widetilde{\delta n}_{\mathbf{k}_\perp}$ are regarded as damped, where the notation $\tilde{A} \equiv A - \langle A\rangle$ is defined. Then, on the lowest-order in K, Eq. (48) reduces to the incompressible-flow condition, which gives

$$\frac{u_{\parallel\mathbf{k}_\perp}}{B} + ic\frac{B_t}{B_p}\frac{k_\perp \phi_{*\mathbf{k}_\perp}}{B^2} \equiv \frac{u_{p\mathbf{k}_\perp}}{B_p} = \left\langle \frac{u_{p\mathbf{k}_\perp}}{B_p}\right\rangle, \tag{64}$$

where Eqs. (A3) and (A4) are used, and $\delta T_{\parallel\mathbf{k}_\perp}$ and $\delta T_{\perp\mathbf{k}_\perp}$ are neglected as higher-order terms in K. Substituting the closure relations, Eqs. (57) and (62), and the incompressibility condition, Eq. (64), into Eq. (50) on the lowest-order in K, we obtain $U_{\mathbf{k}_\perp} = \langle u_{p\mathbf{k}_\perp}/B_p\rangle$ and

$$\left\langle \frac{u_{\parallel\mathbf{k}_\perp}}{B}\right\rangle = iK\frac{T}{m}(\beta_1 - \langle B^{-2}\rangle)\frac{e\phi_{*\mathbf{k}_\perp}}{T} + \beta_1\langle B u_{\parallel\mathbf{k}_\perp}(t=0)\rangle + \frac{1}{n_0}\left\langle \int d^3v F_0 R_{\mathbf{k}_\perp}(t)\overline{\left(\frac{v_\parallel}{B}\right)}\right\rangle, \tag{65}$$

which can also be derived from using Eq. (51) instead of Eq. (50). Now, we combine Eq. (65) with Eq. (63) and take its time integral to obtain

$$\begin{aligned}\langle \delta n_{\mathbf{k}_\perp}^{(g)}(t)\rangle + K^2\frac{T}{m}(\langle B^{-2}\rangle - \beta_1)n_0\frac{e\phi_{*\mathbf{k}_\perp}(t)}{T} &= \langle \delta n_{\mathbf{k}_\perp}^{(g)}(0)\rangle + iKn_0\left\langle \frac{u_{\parallel\mathbf{k}_\perp}(0)}{B}\right\rangle - i\beta_1 K n_0\langle B u_{\parallel\mathbf{k}_\perp}(t=0)\rangle + \left\langle \int d^3v F_0 R_{\mathbf{k}_\perp}(t)\left\{1 + iK\left[\left(\frac{v_\parallel}{B}\right) - \overline{\left(\frac{v_\parallel}{B}\right)}\right]\right\}\right\rangle \\ &= \left\langle \int d^3v\{1 + iK[(v_\parallel/B) - \overline{(v_\parallel/B)}]\}[\delta f_{\mathbf{k}_\perp}^{(g)}(0) + F_0 R_{\mathbf{k}_\perp}(t)]\right\rangle,\end{aligned} \tag{66}$$

where Eqs. (A14) and (A15) are used. The above balance equation derived from the kinetic-fluid model will be used later to describe the long-time zonal-flow evolution.

D. Application to ITG-mode-driven zonal flows

Let us consider the wave-number region $k_\perp a_i < 1$ and present the kinetic-fluid equations to describe zonal flows in the ITG turbulence. Representing the perturbed electron density by $\delta n_{e\mathbf{k}_\perp} = n_0 e(\phi_{\mathbf{k}_\perp} - \langle\phi_{\mathbf{k}_\perp}\rangle)/T_e$ and approximating the even part of the perturbed ion gyrocenter distribution function $\delta f_{i\mathbf{k}_\perp}^{(g)}$ by $\delta f_{i\mathbf{k}_\perp}^{(\text{even})} = F_{i0}[\delta n_{i\mathbf{k}_\perp}^{(g)}/n_0 + (\delta T_{i\parallel\mathbf{k}_\perp}/T_i)(m_i v_\parallel^2/2T_i - 1/2) + (\delta T_{i\perp\mathbf{k}_\perp}/T_i)(m_i v_\perp^2/2T_i - 1)]$ in Eq. (3), the quasineutrality condition is given by

$$e^{-b_i/2}\left(\frac{\delta n_{i\mathbf{k}_\perp}^{(g)}}{n_0} - \frac{b_i}{2}\frac{\delta T_{i\perp\mathbf{k}_\perp}}{T_i}\right) - \frac{e\phi_{\mathbf{k}_\perp}}{T_i}[1 - \Gamma_0(b_i)] = \frac{e}{T_e}(\phi_{\mathbf{k}_\perp} - \langle\phi_{\mathbf{k}_\perp}\rangle). \tag{67}$$

We can divide Eq. (67) into the flux-surface-average part and the remainder part to obtain

$$\frac{e\langle\phi_{\mathbf{k}_\perp}\rangle}{T_i} = \left\langle e^{-b_i/2}\frac{\delta n_{i\mathbf{k}_\perp}^{(g)}/n_0 - (b_i/2)\delta T_{i\perp\mathbf{k}_\perp}/T_i}{T_i/T_e + 1 - \Gamma_0(b_i)}\right\rangle \times \left\langle \frac{1 - \Gamma_0(b_i)}{T_i/T_e + 1 - \Gamma_0(b_i)}\right\rangle^{-1}, \tag{68}$$

$$\frac{e\tilde{\phi}_{\mathbf{k}_\perp}}{T_i} \equiv \frac{e}{T_i}(\phi_{\mathbf{k}_\perp} - \langle\phi_{\mathbf{k}_\perp}\rangle) = \left(\frac{T_i}{T_e} + 1 - \Gamma_0(b_i)\right)^{-1}\left[e^{-b_i/2}\left(\frac{\delta n_{i\mathbf{k}_\perp}^{(g)}}{n_0} - \frac{b_i}{2}\frac{\delta T_{i\perp\mathbf{k}_\perp}}{T_i}\right) - \{1 - \Gamma_0(b_i)\}\frac{e\langle\phi_{\mathbf{k}_\perp}\rangle}{T_i}\right]. \tag{69}$$

Finally, the kinetic-fluid equations for the ITG-mode-driven zonal flow are given by combining Eq. (67) with Eqs. (48)–(51) for the ion fluid variables $(\delta n_{i\mathbf{k}_\perp}^{(g)}, u_{i\parallel\mathbf{k}_\perp}, \delta p_{i\parallel\mathbf{k}_\perp}, \delta p_{i\perp\mathbf{k}_\perp})$, where the closure relations shown in Eqs. (57), (61), and (62), are used for the third- and fourth-order ion variables. We should note that these equations contain nonlinearity sources as unknown terms which result from nonlinear coupling of nonzonal modes (i.e., modes with nonzero toroidal mode numbers). Thus, we still need to present ion kinetic-fluid equations for nonzonal modes in order to construct a complete closed set of equations to self-consistently determine the zonal flows and the ITG turbulence. It is shown by using Eqs. (67) and (63) that, for $k_\perp a_i \ll 1$, the same ion toroidal angular momentum balance as given in Eq. (17) from the kinetic model can also be derived from the kinetic-fluid model.

Now, in order to see how a long-time zonal-flow evolution is determined by our kinetic-fluid model, we make use of $\phi_{\mathbf{k}_\perp} = \langle \phi_{\mathbf{k}_\perp} \rangle$ and $k_\perp a_i \ll 1$ in Eq. (67) to obtain $\delta n_{i\mathbf{k}_\perp}^{(g)} = (k_\perp^2 a_i^2) e\phi_{\mathbf{k}_\perp}/T_i$ which is substituted into Eq. (66). Then, we obtain

$$
\begin{aligned}
n_0 \left[\langle k_\perp^2 a_i^2 \rangle + K_i^2 \frac{T_i}{m_i} (\langle B^{-2} \rangle - \beta_1) \right] \frac{e\phi_{\mathbf{k}_\perp}(t)}{T_i} \\
= \left\langle \int d^3v \{ 1 + iK_i [(v_\parallel / B) - \overline{(v_\parallel/B)}] \} \right. \\
\left. \times \{ \delta f_{i\mathbf{k}_\perp}^{(g)}(0) + F_{i0} R_{i\mathbf{k}_\perp}(t) \} \right\rangle ,
\end{aligned} \tag{70}
$$

which is the same result as derived from the gyrokinetic model in Eq. (19). Also, combining Eqs. (64) and (65) with Eq. (70), we can immediately write the poloidal and parallel components of the ion long-time zonal flow in terms of the nonlinear source and initial-condition terms, which agree with the kinetic results in Sec. II C 1. Thus, our kinetic-fluid model can correctly predict the long-time response of the zonal flow to the initial perturbation and the ITG turbulence source.

With respect to the short-time zonal-flow response, the dispersion relation of the GAM oscillations is derived from the kinetic-fluid equations as shown in Appendix B, where we find that the kinetic-fluid model gives a good approximation to the GAM frequency predicted from the kinetic model[21–23] while the rigorous kinetic GAM damping rate is not approximated as well because the resonant ions' population is not accurately taken into account by the closure relations in Eq. (61).

E. Application to ETG-mode-driven zonal flows

Here, we take the wave-number regions $a_i^{-1} \ll k_\perp < a_e^{-1}$ relevant to zonal flows in the ETG turbulence. Then, we represent the perturbed ion density by $\delta n_{i\mathbf{k}_\perp} = -n_0 e\phi_{\mathbf{k}_\perp}/T_i$ and the even part of the perturbed electron gyrocenter distribution function $\delta f_{e\mathbf{k}_\perp}^{(g)}$ by $\delta f_{e\mathbf{k}_\perp}^{(\mathrm{even})} = F_{e0}[\delta n_{e\mathbf{k}_\perp}^{(g)}/n_0 + (\delta T_{e\parallel \mathbf{k}_\perp}/T_e)(m_e v_\parallel^2/2T_e - 1/2) + (\delta T_{e\perp \mathbf{k}_\perp}/T_e)(m_e v_\perp^2/2T_e - 1)]$ in Eq. (3) to write Poisson's equation as

$$
\begin{aligned}
e^{-b_e/2} \left(\frac{\delta n_{e\mathbf{k}_\perp}^{(g)}}{n_0} - \frac{b_e}{2} \frac{\delta T_{e\perp\mathbf{k}_\perp}}{T_e} \right) \\
+ \frac{e\phi_{\mathbf{k}_\perp}}{T_e} \left(\frac{T_e}{T_i} + 1 - \Gamma_0(b_e) + k_\perp^2 \lambda_{\mathrm{De}}^2 \right) = 0 .
\end{aligned} \tag{71}
$$

In the same way as in Eq. (67), we divide Eq. (71) into the flux-surface-average part and the remainder part to obtain

$$
\frac{e\langle \phi_{\mathbf{k}_\perp} \rangle}{T_e} = - \left\langle e^{-b_e/2} \frac{\delta n_{e\mathbf{k}_\perp}^{(g)}/n_0 - (b_e/2)\delta T_{e\perp\mathbf{k}_\perp}/T_e}{T_e/T_i + 1 - \Gamma_0(b_e) + k_\perp^2 \lambda_{\mathrm{De}}^2} \right\rangle , \tag{72}
$$

$$
\begin{aligned}
\frac{e\tilde{\phi}_{\mathbf{k}_\perp}}{T_e} &\equiv \frac{e}{T_e} (\phi_{\mathbf{k}_\perp} - \langle \phi_{\mathbf{k}_\perp} \rangle) \\
&= - \left(\frac{T_e}{T_i} + 1 - \Gamma_0(b_e) + k_\perp^2 \lambda_{\mathrm{De}}^2 \right)^{-1} \\
&\quad \times e^{-b_e/2} \left(\frac{\delta n_{e\mathbf{k}_\perp}^{(g)}}{n_0} - \frac{b_e}{2} \frac{\delta T_{e\perp\mathbf{k}_\perp}}{T_e} \right) - \frac{e\langle \phi_{\mathbf{k}_\perp} \rangle}{T_e} .
\end{aligned} \tag{73}
$$

Now, the kinetic-fluid equations for the ETG-mode-driven zonal flow are given by combining Eq. (71) with Eqs. (48)–(51) for the electron fluid variables $(\delta n_{e\mathbf{k}_\perp}^{(g)}, u_{e\parallel\mathbf{k}_\perp}, \delta p_{e\parallel\mathbf{k}_\perp}, \delta p_{e\perp\mathbf{k}_\perp})$, where the closure relations shown in Eqs. (57), (61), and (62), are used for the third- and fourth-order electron variables. We here repeat that these equations contain nonlinearity sources as unknown terms which result from nonlinear coupling of nonzonal modes and that it is necessary to present electron kinetic-fluid equations for nonzonal modes in order to construct a complete closed set of equations to self-consistently determine the zonal flows and the ETG turbulence.

Parallel to Eq. (70), a long-time electron zonal-flow potential in the ETG turbulence is obtained by combining Eq. (66) with $e^{-b_e/2}\delta n_{e\mathbf{k}_\perp}^{(g)} = -[T_e/T_i + k_\perp^2(a_e^2 + \lambda_{\mathrm{De}}^2)] e\phi_{\mathbf{k}_\perp}/T_e$ as

$$
\begin{aligned}
&\left[\frac{T_e}{T_i} + \langle k_\perp^2 (a_e^2 + \lambda_{\mathrm{De}}^2) \rangle + K_e^2 \frac{T_e}{m_e} \right. \\
&\quad \left. \times \left(1 + \frac{T_e}{T_i} \right) (\langle B^{-2} \rangle - \beta_1) \right] \frac{e\phi_{\mathbf{k}_\perp}(t)}{T_e} \\
&= \left(\frac{T_e}{T_i} + \langle k_\perp^2 (a_e^2 + \lambda_{\mathrm{De}}^2) \rangle \right) \frac{e\phi_{\mathbf{k}_\perp}(0)}{T_e} - \frac{\langle e^{-b_e/2} \delta n_{e\mathbf{k}_\perp}^{(s)}(t) \rangle}{n_0} \\
&\quad - iK_e (\langle \{ u_{e\parallel\mathbf{k}_\perp}(0) + u_{e\parallel\mathbf{k}_\perp}^{(s)}(t) \} / B \rangle \\
&\quad - \beta_1 \langle \{ u_{e\parallel\mathbf{k}_\perp}(0) + u_{e\parallel\mathbf{k}_\perp}^{(s)}(t) \} B \rangle) ,
\end{aligned} \tag{74}
$$

which coincides with Eq. (36). In deriving Eq. (74), terms up to $\mathcal{O}(k_\perp^2 a_e^2)$ are kept and $(-b_e/2)(\delta T_{e\perp\mathbf{k}_\perp}/T_e)$ is neglected as a higher-order term in $k_\perp a_e$. Also, using Eqs. (64) and (65), we can get the same expressions for all components of the long-time electron zonal flow as those derived from the gyrokinetic model. Thus, the present kinetic-fluid model properly reproduces the gyrokinetic result in Sec. II C 2 for the long-time response of the zonal flow to the initial perturbation and the ETG turbulence source.

IV. NUMERICAL RESULTS

In order to further examine the validity of the kinetic-fluid model of zonal flows presented in the previous section, numerical results from our model are compared with those from gyrokinetic simulation. We consider large-aspect-ratio tokamaks, in which flux surfaces have concentric circular cross sections. The magnetic-field strength is written as $B = B_0(1-\epsilon \cos\theta)$ with $\epsilon \equiv r/R_0 \ll 1$, where R_0 denotes the distance from the toroidal major axis to the magnetic axis, r is the minor radius, and θ is the poloidal angle.

A. Zonal flows in the wave number region relevant to ITG turbulence

Here, we are concerned with zonal flows generated by ITG turbulence and take the low radial wave numbers $k_\perp a_i < 1$. The linearized version of the ion gyrokinetic equation given by Eq. (1) and the quasineutrality condition ($k_\perp \lambda_{De} = 0$) in Eq. (3) with the perturbed electron density given by $\delta n_{e\mathbf{k}_\perp} = n_0 e(\phi_{\mathbf{k}_\perp} - \langle \phi_{\mathbf{k}_\perp}\rangle)/T_e$ are solved by the toroidal flux-tube gyrokinetic Vlasov (GKV) code[11] to obtain the response of the zonal-flow potential to the initial perturbation. As mentioned in Sec. II A, this solution of the linear initial-value also describes the zonal-flow response to the nonlinear source term. For comparison, we also numerically solve the kinetic-fluid equations shown in Eqs. (B11)–(B16), where a further assumption in Eq. (B9) is made and $\mathcal{O}(\epsilon^2)$ terms are neglected. Results from the gyrokinetic simulation and the kinetic-fluid simulation for $q=1.5$, $\tau_e \equiv T_e/T_i = 1$, and $\epsilon = 0.1$ are plotted by solid circular symbols and solid curves, respectively, in Fig. 1, where the residual zonal-flow level predicted by Rosenbluth and Hinton [see Eq. (29)] is also plotted by the horizontal dashed line. Here, the initial condition is given by $\delta f^{(g)}_{i\mathbf{k}_\perp}(0) = (\delta n^{(g)}_{i\mathbf{k}_\perp}(0)/n_0)F_{i0}$ with $\delta n^{(g)}_{i\mathbf{k}_\perp}(0)/n_0 = [1-\Gamma_0(b_i)]e\phi_{\mathbf{k}_\perp}(0)/T_i$. The normalized radial wave numbers $k_r a_i = 0.0654$, 0.131, and 0.196 are used in Figs. 1(a)–1(c), respectively. We see a good agreement between the gyrokinetic and fluid simulation results in that both of them show the convergence to the Rosenbluth-Hinton zonal-flow level as well as nearly the same frequency of the GAM oscillations. However, the gyrokinetic simulation results show the GAM damping rate that depends on the radial wave number while this dependence is not seen in the fluid simulation.

It is confirmed that the real frequency and the damping rate of the GAM oscillations shown by the fluid simulation are well predicted by the analytical expression in Eq. (D7). This formula shows no dependence on the radial wave number and its real part gives a good approximation to the GAM frequency obtained by the gyrokinetic simulation. However, its imaginary part cannot accurately reproduce the GAM damping shown in the gyrokinetic simulation because the present kinetic-fluid model misses the correct resonant ion parallel velocity (see the statements at the end of Appendix D). The dependence of the GAM damping rate on the radial wave number can be explained as an effect of finite widths of passing-particle orbits.[9,21]

The agreement between the gyrokinetic and fluid simulation results with respect to the GAM damping rates found in Fig. 1(b) is an accidental one while we believe that, even if such differences in the GAM damping rates as seen in Figs. 1(a) and 1(c) exist, our kinetic-fluid model is still useful because it reproduces the gyrokinetic residual zonal-flow level, which is more of a critical factor to regulate the turbulent transport than the GAM oscillations.

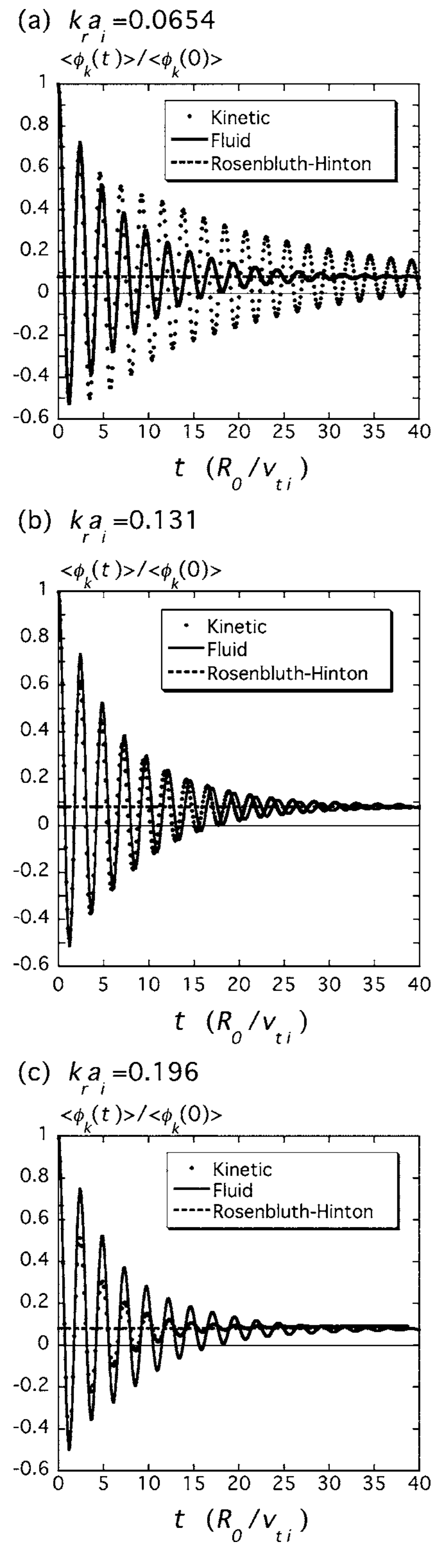

FIG. 1. Time evolution of the zonal-flow potential for $k_r a_i = 0.0654$ (a), 0.131 (b), and 0.196 (c). Here, $q=1.5$, $\tau_e \equiv T_e/T_i = 1$, and $\epsilon = 0.1$ are used. Results from the gyrokinetic simulation and the kinetic-fluid simulation are plotted by solid circular symbols and solid curves, respectively. The residual zonal-flow level predicted by Rosenbluth and Hinton [see Eq. (29)] is also plotted by the horizontal dashed line.

B. Zonal flows in the wave number region relevant to ETG turbulence

Now, let us consider the case of zonal flows generated by the ETG turbulence and assume the radial wave numbers to be in the region, $a_i^{-1} \ll k_r < a_e^{-1}$. Then, the gyrokinetic Vlasov simulation is done to solve the linearized version of the electron gyrokinetic equation given by Eq. (1) and the quasineutrality condition obtained from Eq. (3) with the perturbed ion density $\delta n_{i\mathbf{k}_\perp} = -n_0 e\phi_{\mathbf{k}_\perp}/T_i$. The initial condition is given by $\delta f^{(g)}_{e\mathbf{k}_\perp}(0) = (\delta n^{(g)}_{e\mathbf{k}_\perp}(0)/n_0)F_{i0}$ with $e^{-b_e/2}\delta n^{(g)}_{e\mathbf{k}_\perp}(0)/n_0 = -[T_e/T_i + 1 - \Gamma_0(b_e)]e\phi_{\mathbf{k}_\perp}(0)/T_e$. Here, $q=1.4$, $\tau_e = T_e/T_i = 1$, $\epsilon=0.18$, and $k_r\lambda_{\mathrm{De}}=0$ are used. Also, the kinetic-fluid model equations described in the end of Appendix C are numerically solved for comparison. The gyrokinetic and fluid simulation results for $k_r a_e = 0.1715$ are shown by solid circular symbols and solid curves, respectively, in Fig. 2(a), where the residual zonal-flow level predicted by Eq. (43) is also plotted by the horizontal dashed line. The residual zonal-flow level is shown as a function of $k_r a_e$ in Fig. 2(b), where open circles, crosses, and a solid curve represent the gyrokinetic, kinetic-fluid results, and the analytical prediction from Eq. (43), respectively. The gyrokinetic and fluid simulation results both show a good agreement with the predicted zonal-flow level. It is now verified that our kinetic-fluid model can correctly reproduce the gyrokinetic long-time zonal-flow response for the radial wave numbers relevant to the ETG turbulence as well.

V. CONCLUSIONS

In this paper, new kinetic-fluid equations are presented, which describe collisionless zonal-flow evolution in tokamak plasmas. Our kinetic-fluid closure model is derived from using the analytical solution of the gyrokinetic equation and it is applied to zonal flows generated by ITG and ETG turbulence. It is analytically verified that, for both radial wave-number regions relevant to the ITG and ETG turbulence, the residual zonal-flow levels predicted by the gyrokinetic model can be correctly reproduced by the kinetic-fluid model as well. Also, the kinetic-fluid equations are used to derive the dispersion relation for the GAM oscillations of the ITG-mode-driven zonal flows.

Furthermore, the validity of the kinetic-fluid model of zonal flows is examined by comparing numerical solutions of the kinetic-fluid equations including our closure model with those of the gyrokinetic equations obtained by the gyrokinetic Vlasov simulation. The response of the zonal flow to the initial perturbation is determined by the gyrokinetic and fluid simulations, which show the same residual zonal-flow level as theoretically predicted for both radial wave-number regions relevant to the ITG and ETG turbulence. This also implies that the closure model can correctly describe the zonal-flow responses to the ITG and ETG turbulence sources [Eqs. (32) and (46)] which indicate the inefficient generation of zonal flows in the ETG turbulence due to the enhancement of their inertia. We also see that the gyrokinetic and fluid simulations show almost the same GAM frequency of the ITG-mode-driven zonal flow although our kinetic-fluid model does not give the radial-wave-number de-

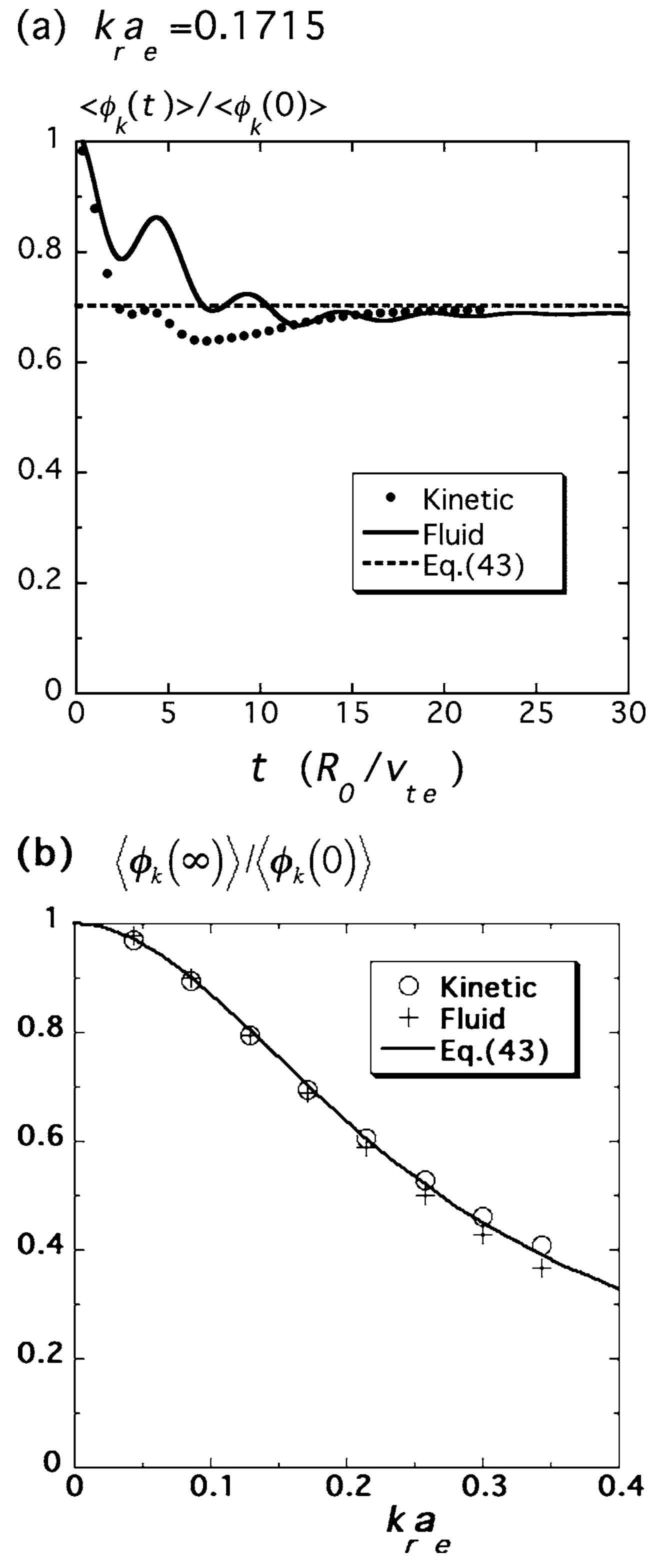

FIG. 2. Time evolution of the zonal-flow potential for $k_r a_e = 0.1715$ (a) and the residual zonal-flow level as a function of $k_r a_e$. Here, $q=1.4$, $\tau_e \equiv T_e/T_i = 1$, $\epsilon=0.18$, and $k_r\lambda_{\mathrm{De}}=0$ are used. Results from the gyrokinetic simulation and the kinetic-fluid simulation are plotted by solid circular symbols and a solid curve, respectively, and the residual zonal-flow level predicted by Eq. (43) is also plotted by the horizontal dashed line in (a). Open circles, crosses, and a solid curve in (b) represent the gyrokinetic, kinetic-fluid results, and the analytical prediction from Eq. (43), respectively.

pendence of the GAM damping rate found by the gyrokinetic model because the exact parallel velocity of ions resonating with the GAM oscillations is not included in the present kinetic-fluid model. Even so, since it is not the GAM but residual zonal flow that is a critical factor to suppress the turbulence, our kinetic-fluid model is expected to be useful for calculation of the same level of turbulent transport as given by the gyrokinetic simulation with less computational costs by performing the nonlinear fluid simulation based on a closed set of equations given by combining our kinetic-fluid zonal-flow model with kinetic-fluid equations for other non-zonal modes. This nonlinear kinetic-fluid simulation is a crucial task from the practical viewpoint for a quick and accurate prediction of anomalous transport.

It should be noted that collisions are another important factor, which is not treated in this paper, to determine the zonal-flow level and accordingly the anomalous transport in both ITG (Ref. 24) and ETG (Ref. 14) turbulence. For closer comparisons to other simulations and experimental studies on the regulation of turbulent transport by zonal flows, extensions of the present work to the collisional case and other toroidal configurations such as helical systems remain as future problems.

ACKNOWLEDGMENTS

This work is supported in part by the Japanese Ministry of Education, Culture, Sports, Science, and Technology, Grant Nos. 16560727 and 17360445 and in part by the NIFS Collaborative Research Program, NIFS06KDAD006, NIFS06KNXN060, and NIFS06KTAT038.

APPENDIX A: INCOMPRESSIBLE ZONAL FLOWS

The zonal flow tangential to the flux surface is generally written as

$$\mathbf{u}_{\mathbf{k}_\perp} = \mathbf{u}_{t\mathbf{k}_\perp} + \mathbf{u}_{p\mathbf{k}_\perp} = u_{\parallel\mathbf{k}_\perp}\mathbf{b} + \mathbf{u}_{\perp\mathbf{k}_\perp}, \tag{A1}$$

where $\mathbf{u}_{t\mathbf{k}_\perp} \equiv u_{t\mathbf{k}_\perp} R\nabla\zeta$ and $\mathbf{u}_{p\mathbf{k}_\perp} \equiv u_{p\mathbf{k}_\perp}\mathbf{B}_p/B_p$ represent the toroidal and poloidal flow components, respectively, while $u_{\parallel\mathbf{k}_\perp}\mathbf{b}$ and $\mathbf{u}_{\perp\mathbf{k}_\perp}$ are the parallel and perpendicular flow components, respectively. The parallel flow component $u_{\parallel\mathbf{k}_\perp} \equiv \mathbf{u}_{\mathbf{k}_\perp}\cdot\mathbf{b}$ and the perpendicular flow component $u_{\perp\mathbf{k}_\perp} \equiv \mathbf{u}_{\mathbf{k}_\perp}\cdot(\mathbf{b}\times\nabla r)/|\nabla r|$ are written in terms of the toroidal and poloidal flow components as

$$\begin{aligned} u_{\parallel\mathbf{k}_\perp} &= (B_t u_{t\mathbf{k}_\perp} + B_p u_{p\mathbf{k}_\perp})/B, \\ u_{\perp\mathbf{k}_\perp} &= (-B_p u_{t\mathbf{k}_\perp} + B_t u_{p\mathbf{k}_\perp})/B. \end{aligned} \tag{A2}$$

Inversely, the toroidal and poloidal flow components are given by

$$\begin{aligned} u_{t\mathbf{k}_\perp} &= (B_t u_{\parallel\mathbf{k}_\perp} - B_p u_{\perp\mathbf{k}_\perp})/B, \\ u_{p\mathbf{k}_\perp} &= (B_p u_{\parallel\mathbf{k}_\perp} + B_t u_{\perp\mathbf{k}_\perp})/B. \end{aligned} \tag{A3}$$

Here, we represent the parallel flow by $u_{\parallel\mathbf{k}_\perp} \equiv n_0^{-1}\int d^3v\,\delta f_{\mathbf{k}_\perp}^{(g)} v_\parallel$ while we take account of the $\mathbf{E}\times\mathbf{B}$ drift velocity $\mathbf{u}_{E\mathbf{k}_\perp} \equiv ick_r\phi_{\mathbf{k}_\perp}\mathbf{b}\times\nabla r/B$ and the perturbed-density-gradient-driven drift velocity $\mathbf{u}_{*\mathbf{k}_\perp} \equiv ik_rT\langle\delta n_{\mathbf{k}_\perp}\rangle\mathbf{b}\times\nabla r/(n_0 m\Omega)$ to express the perpendicular flow by

$$\begin{aligned} u_{\perp\mathbf{k}_\perp} &\equiv (\mathbf{u}_{E\mathbf{k}_\perp} + \mathbf{u}_{*\mathbf{k}_\perp})\cdot(\mathbf{b}\times\nabla r)/|\nabla r| \\ &= i\frac{k_\perp T}{m\Omega}\left(\frac{e\phi_{\mathbf{k}_\perp}}{T} + \frac{\langle\delta n_{\mathbf{k}_\perp}\rangle}{n_0}\right) \equiv ick_\perp\phi_{*\mathbf{k}_\perp}/B, \end{aligned} \tag{A4}$$

where $e\phi_{*\mathbf{k}_\perp}/T \equiv e\phi_{\mathbf{k}_\perp}/T + \langle\delta n_{\mathbf{k}_\perp}\rangle/n_0$ is defined. Equation (A4) is consistent with the perpendicular flow derived from taking the perpendicular velocity moment of the perturbed particle distribution function $\delta f_{\mathbf{k}_\perp}$ in Eq. (2) up to the leading order in $k_\perp\rho$. Here, we should note that subscripts to represent particle species are omitted although $\phi_{*\mathbf{k}_\perp}$ has species-dependence such that $\phi_{i*\mathbf{k}_\perp} \equiv \phi_{\mathbf{k}_\perp} + (T_i/e)\langle\delta n_{i\mathbf{k}_\perp}\rangle/n_0$ and $\phi_{e*\mathbf{k}_\perp} \equiv \phi_{\mathbf{k}_\perp} - (T_e/e)\langle\delta n_{e\mathbf{k}_\perp}\rangle/n_0$. As shown in Secs. II C 1 and II C 2, contribution of the perturbed-density-gradient-driven velocity to the perpendicular velocity can be neglected for the wave number region $k_\perp a_i < 1$ $[a_i \equiv (T_i/m_i)^{1/2}/\Omega_i]$ relevant to the ITG turbulence although it cannot for $1/a_i \ll k_\perp < 1/a_e$ $[a_e \equiv (T_e/m_e)^{1/2}/|\Omega_e|]$ relevant to the ETG turbulence. Thus, we redefine $\phi_{*\mathbf{k}_\perp}$ by $\phi_{i*\mathbf{k}_\perp} = \phi_{\mathbf{k}_\perp}$ for $k_\perp a_i < 1$ and $\phi_{e*\mathbf{k}_\perp} \equiv \phi_{\mathbf{k}_\perp} - (T_e/e)\langle\delta n_{e\mathbf{k}_\perp}\rangle/n_0$ for $1/a_i \ll k_\perp < 1/a_e$.

We should recall that $\phi_{\mathbf{k}_\perp} = \langle\phi_{\mathbf{k}_\perp}\rangle$, $RB_t = I$, and $(B_t/B_p)Bu_{\perp\mathbf{k}_\perp} = ick_r I\phi_{*\mathbf{k}_\perp}/(d\psi/dr)$ are all constant on the flux surface. Then, Eqs. (A2) and (A3) yield

$$\langle R^2\rangle\langle(B_t/B_p)Bu_{\perp\mathbf{k}_\perp}\rangle = -\langle RB_t\rangle\langle Ru_{t\mathbf{k}_\perp}\rangle + \langle RB_t\rangle^2\langle u_{p\mathbf{k}_\perp}/B_p\rangle,$$

$$\langle B^2(u_{p\mathbf{k}_\perp}/B_p)\rangle = \langle Bu_{\parallel\mathbf{k}_\perp}\rangle + \langle(B_t/B_p)Bu_{\perp\mathbf{k}_\perp}\rangle,$$

which are used to derive

$$\begin{aligned} \langle Bu_{\parallel\mathbf{k}_\perp}\rangle &= \frac{\langle RB_t\rangle}{\langle R^2\rangle}\langle Ru_{t\mathbf{k}_\perp}\rangle + (1+2\hat{q}^2)\langle B_p^2\rangle\langle u_{p\mathbf{k}_\perp}/B_p\rangle \\ &\quad + \langle B^2(u_{p\mathbf{k}_\perp}/B_p)\rangle - \langle B^2\rangle\langle u_{p\mathbf{k}_\perp}/B_p\rangle. \end{aligned} \tag{A5}$$

Here, $\hat{q}$ is defined by[25]

$$\hat{q}^2 \equiv \frac{1}{2\langle B_p^2\rangle}\left[\langle B_t^2\rangle - \frac{\langle RB_t\rangle^2}{\langle R^2\rangle}\right], \tag{A6}$$

which reduces to the square of the safety factor q in the large-aspect-ratio limit.

Using Eq. (15), we find that the lowest-order parallel flow $u_{\parallel\mathbf{k}_\perp}(t) \equiv n_0^{-1}\int d^3v\,\delta f_{\mathbf{k}_\perp}^{(g)}(t)v_\parallel$ in $k_\perp\rho$ is expressed in the form, which is consistent with Eq. (A3), as

$$\begin{aligned} u_{\parallel\mathbf{k}_\perp}(t) &= [-B_t u_{\perp\mathbf{k}_\perp}(t) + Bu_{p\mathbf{k}_\perp}(t)]/B_p \\ &= [-ic(B_t/B)k_\perp\phi_{*\mathbf{k}_\perp}(t) + Bu_{p\mathbf{k}_\perp}(t)]/B_p, \end{aligned} \tag{A7}$$

where $u_{p\mathbf{k}_\perp}(t)$ is given by

$$\begin{aligned} u_{p\mathbf{k}_\perp}(t)/B_p &= i\beta_1 c(B_t/B_p)k_\perp\phi_{*\mathbf{k}_\perp}(t) + \alpha_{\mathbf{k}_\perp} \\ &= i\beta_1 cIk_r\phi_{*\mathbf{k}_\perp}(t)/(d\psi/dr) + \alpha_{\mathbf{k}_\perp}, \end{aligned} \tag{A8}$$

and $\langle\delta n_{\mathbf{k}_\perp}\rangle$, which is necessary to define $\phi_{*\mathbf{k}_\perp}$ for electrons in the case of the ETG turbulence, is represented by

$$\langle \delta n_{\mathbf{k}_\perp} \rangle = \int d^3v \{ \overline{\delta f^{(g)}_{\mathbf{k}_\perp}(0)} + F_0 \overline{R_{\mathbf{k}_\perp}(t)} \}. \tag{A9}$$

The validity of Eq. (A9) for electrons is verified in Sec. II C. Here, $\alpha_{\mathbf{k}_\perp}$ and β_1 are defined by

$$\alpha_{\mathbf{k}_\perp} \equiv \frac{1}{n_0 B} \int d^3v \{ \overline{\delta f^{(g)}_{\mathbf{k}_\perp}(0)} + F_0 \overline{R_{\mathbf{k}_\perp}(t)} \} v_\parallel, \tag{A10}$$

and

$$\beta_1 \equiv \frac{3}{2} \int_0^{1/B_M} \frac{d\lambda}{\langle B/(1-\lambda B)^{1/2} \rangle}, \tag{A11}$$

respectively, where B_M denotes the maximum field strength over the flux surface. It is found from Eqs. (A8)–(A11) that $(u_{p\mathbf{k}_\perp}/B_p)$, $\alpha_{\mathbf{k}_\perp}$, and β_1 are all constant on the flux surface. Thus, as seen in the standard neoclassical theory,[25] the lowest-order flow $\mathbf{u}_{\mathbf{k}_\perp}$ satisfies the incompressibility condition,

$$\nabla \cdot \mathbf{u}_{\mathbf{k}_\perp} = \mathbf{B}_p \cdot \nabla (u_{p\mathbf{k}_\perp}/B_p) = 0. \tag{A12}$$

This seems a natural result because here we consider only the slow time evolution, in which fast compressional waves such as GAMs are excluded. Also, for the incompressible flow, the last two terms in Eq. (A5) cancel with each other and we have

$$\langle B u_{\parallel \mathbf{k}_\perp} \rangle = \frac{\langle R B_t \rangle}{\langle R^2 \rangle} \langle R u_{t\mathbf{k}_\perp} \rangle + (1 + 2\hat{q}^2) \langle B_p^2 \rangle \langle u_{p\mathbf{k}_\perp}/B_p \rangle. \tag{A13}$$

For $k_\perp \rho \ll 1$, we assume that $\delta f^{(g)}_{\mathbf{k}_\perp}(0)$ and $F_0 R_{\mathbf{k}_\perp}(t)$ are both given in the form of the shifted Maxwellian by

$$\delta f^{(g)}_{\mathbf{k}_\perp}(0) = F_0 \left[\frac{\delta n^{(g)}_{\mathbf{k}_\perp}(0)}{n_0} + \frac{m}{T} u_{\parallel \mathbf{k}_\perp}(0) v_\parallel \right], \tag{A14}$$

and

$$F_0 R_{\mathbf{k}_\perp}(t) = F_0 \left[\frac{\delta n^{(s)}_{\mathbf{k}_\perp}(t)}{n_0} + \frac{m}{T} u^{(s)}_{\parallel \mathbf{k}_\perp}(t) v_\parallel \right], \tag{A15}$$

respectively. Then, Eqs. (A9) and (A10) are rewritten as

$$\langle \delta n_{\mathbf{k}_\perp} \rangle = \delta n^{(g)}_{\mathbf{k}_\perp}(0) + \delta n^{(s)}_{\mathbf{k}_\perp}(t) \tag{A16}$$

and

$$\alpha_{\mathbf{k}_\perp} = \beta_1 \langle B \{ u_{\parallel \mathbf{k}_\perp}(0) + u^{(s)}_{\parallel \mathbf{k}_\perp}(t) \} \rangle, \tag{A17}$$

respectively.

APPENDIX B: KINETIC-FLUID EQUATIONS OF ITG-MODE-DRIVEN ZONAL FLOWS IN LARGE-ASPECT-RATIO TOKAMAKS

This Appendix presents the kinetic-fluid equations of ITG-mode-driven zonal flows for large-aspect-ratio tokamaks, in which flux surfaces have concentric circular cross sections and the magnetic-field strength is written as $B = B_0(1 - \epsilon \cos\theta)$ with $\epsilon \equiv r/R_0 \ll 1$. As usual, R_0 denotes the distance from the toroidal major axis to the magnetic axis, r is the minor radius, and θ is the poloidal angle. Then, Eqs. (21) and (59) can be approximately written as $\beta_1 = B_0^{-2}(1 - C\epsilon^{3/2})$ and $\beta_2 = B_0^{-3}(1 - \frac{5}{2} C\epsilon^{3/2})$, respectively, where $C \simeq 1.6$ [see Eq. (27)]. Here, we assume the long radial wavelength $k_\perp a_i < 1$, and for simplicity, we use the following normalization:

$$\left[\frac{v_{ti} t}{R_0 q}, \frac{e\phi_{\mathbf{k}_\perp}}{T_i}, \frac{\delta n^{(g)}_{i\mathbf{k}_\perp}}{n_0}, \frac{u_{i\parallel \mathbf{k}_\perp}}{v_{ti}}, \frac{\delta p_{i\parallel \mathbf{k}_\perp}}{p_{i0}}, \frac{\delta p_{i\perp \mathbf{k}_\perp}}{p_{i0}} \right] \to [t, \phi, \delta n^{(g)}_i, u_{i\parallel}, \delta p_{i\parallel}, \delta p_{i\perp}],$$

$$\left[\frac{q_{i\parallel \mathbf{k}_\perp}}{p_{i0} v_{ti}}, \frac{q_{i\perp \mathbf{k}_\perp}}{p_{i0} v_{ti}}, \frac{\delta r_{i\parallel\parallel \mathbf{k}_\perp}}{p_{i0} v_{ti}^2}, \frac{\delta r_{i\parallel\perp \mathbf{k}_\perp}}{p_{i0} v_{ti}^2}, \frac{\delta r_{i\perp\perp \mathbf{k}_\perp}}{p_{i0} v_{ti}^2} \right] \to [q_{i\parallel}, q_{i\perp}, \delta r_{i\parallel\parallel}, \delta r_{i\parallel\perp}, \delta r_{i\perp\perp}], \tag{B1}$$

$$\left[\frac{R_0 q \mathcal{N}_{i0\mathbf{k}_\perp}}{n_0 v_{ti}}, \frac{R_0 q \mathcal{N}_{i1\mathbf{k}_\perp}}{p_{i0}}, \frac{R_0 q \mathcal{N}_{i2\parallel \mathbf{k}_\perp}}{p_{i0} v_{ti}}, \frac{R_0 q \mathcal{N}_{i2\perp \mathbf{k}_\perp}}{p_{i0} v_{ti}}, \right] \to [\mathcal{N}_{i0}, \mathcal{N}_{i1}, \mathcal{N}_{i2\parallel}, \mathcal{N}_{i2\perp}]$$

where q is the safety factor and $v_{ti} \equiv (T_i/m_i)^{1/2}$. Then, from Eqs. (48)–(51) and (67), we obtain the perturbed ion gyrocenter density equation,

$$\frac{\partial \delta n^{(g)}_i}{\partial t} + \frac{\partial u_{i\parallel}}{\partial \theta} - \epsilon u_{i\parallel} \sin\theta = i(k_r a_i q) \sin\theta [\delta p_{i\parallel} + \delta p_{i\perp} + \phi e^{-b_i/2}(2 - b_i/2)] + \mathcal{N}_{i0}, \tag{B2}$$

the parallel ion momentum balance equation,

$$\frac{\partial u_{i\parallel}}{\partial t} + \frac{\partial \delta p_{i\parallel}}{\partial \theta} + \epsilon \sin\theta (\delta p_{i\perp} - \delta p_{i\parallel}) = i(k_r a_i q) \sin\theta (q_{i\parallel} + q_{i\perp} + 4u_{i\parallel}) - \frac{\partial (e^{-b_i/2}\phi)}{\partial \theta} + \frac{b_i}{2} e^{-b_i/2} \epsilon \phi \sin\theta + \mathcal{N}_{i1}, \tag{B3}$$

the perturbed parallel ion pressure equation,

$$\frac{\partial \delta p_{i\parallel}}{\partial t} + \frac{\partial (q_{i\parallel} + 3u_{i\parallel})}{\partial \theta} + \epsilon \sin\theta (2q_{i\perp} - q_{i\parallel} - u_{i\parallel}) = i(k_r a_i q) \sin\theta [\delta r_{i\parallel\parallel} + \delta r_{i\parallel\perp} + \phi e^{-b_i/2}(4 - b_i/2)] + \mathcal{N}_{i2\parallel}, \tag{B4}$$

the perturbed perpendicular ion pressure equation,

$$\frac{\partial \delta p_{i\perp}}{\partial t} + \frac{\partial (q_{i\perp} + u_{i\parallel})}{\partial \theta} - 2\epsilon \sin\theta (q_{i\perp} + u_{i\parallel}) = i(k_r a_i q) \sin\theta [\delta r_{i\parallel\perp} + \delta r_{i\perp\perp} + \phi e^{-b_i/2} \times (3 - 3b_i/2 + b_i^2/8)] + \mathcal{N}_{i2\perp}, \tag{B5}$$

and the quasineutrality condition,

$$e^{-b_i/2}\left(\delta n_i^{(g)} - \frac{b_i}{2}\delta T_{i\perp}\right) - \phi[1-\Gamma_0(b_i)] = \frac{1}{\tau_e}(\phi - \langle\phi\rangle), \tag{B6}$$

where $\tau_e \equiv T_e/T_i$, $b_i \equiv k_r^2 a_i^2$, $a_i \equiv v_{ti}/\Omega_{i0}$, and $\Omega_{i0} \equiv eB_0/(m_i c)$. The closure relations for the parallel ion heat fluxes $q_{i\|}=q_{i\|}^{(l)}+q_{i\|}^{(s)}$ and $q_{i\perp}=q_{i\perp}^{(l)}+q_{i\perp}^{(s)}$ are given by

$$q_{i\|}^{(l)} = -2q_{i\perp}^{(l)} = 2U_i\left(\hat{B} - \frac{\hat{\beta}_2}{\hat{\beta}_1}\hat{B}^2\right),$$

$$U_i = \hat{\beta}_1(\hat{\beta}_1-1)^{-1}\left\{\left\langle\frac{u_{i\|}}{\hat{B}}\right\rangle - \left\langle\hat{B}\left[u_{i\|}(t=0) + \int_0^t dt'\mathcal{N}_{i1}(t')\right]\right\rangle\right\}, \tag{B7}$$

$$q_{i\|m}^{(s)} = -2\left(\frac{2}{\pi}\right)^{1/2} i\frac{m}{|m|}\delta T_{i\|m},$$

$$q_{i\perp m}^{(s)} = -\left(\frac{2}{\pi}\right)^{1/2} i\frac{m}{|m|}\delta T_{i\perp m},$$

where $\delta T_{i\|} \equiv \delta p_{i\|} - \delta n_{i\|}^{(g)}$, $\delta T_{i\perp} \equiv \delta p_{i\perp} - \delta n_{i\|}^{(g)}$, $\hat{B} \equiv B/B_0 \equiv 1 - \epsilon\cos\theta$, $\hat{\beta}_1 \equiv 1 - C\epsilon^{3/2}$, $\hat{\beta}_2 \equiv 1 - \frac{5}{2}C\epsilon^{3/2}$, and the integer m represents the mode number in the Fourier series of arbitrary periodic function of θ as given by $g(\theta)=\Sigma_m g_m e^{im\theta}$. The fourth-order ion fluid variables are given by

$$[\delta r_{i\|\|}, \delta r_{i\|\perp}, \delta r_{i\perp\perp}] = \delta n_i^{(g)}[3,1,2]. \tag{B8}$$

Now, further simplifications are done by neglecting $\mathcal{O}(\epsilon^2)$ terms and representing the poloidal-angle dependence of an arbitrary fluid variable $Q(r,\theta)$ appearing in Eqs. (B2)–(B8) as

$$Q(r,\theta) = Q_0(r) + Q_c(r)\cos\theta + Q_s(r)\sin\theta. \tag{B9}$$

Hereafter, the subscripts 0, c, and s are used to represent constant, cosine, and sine parts, respectively. Then, the flux-surface average of Q is written as

$$\langle Q\rangle = \frac{\oint Q\,dl/B}{\oint dl/B} = \oint\frac{d\theta}{2\pi}(1+\epsilon\cos\theta)Q = Q_0 + \frac{\epsilon}{2}Q_c. \tag{B10}$$

From Eqs. (B2)–(B6), we obtain the perturbed ion gyrocenter density equations,

$$\frac{\partial\delta n_{i0}^{(g)}}{\partial t} - \frac{\epsilon}{2}u_{i\|s} = \frac{i}{2}(k_r a_i q)[\delta p_{i\|s} + \delta p_{i\perp s} + \phi_s e^{-b_i/2}\times(2-b_i/2)] + (\mathcal{N}_{i0})_0,$$

$$\frac{\partial\delta n_{ic}^{(g)}}{\partial t} + u_{i\|s} = (\mathcal{N}_{i0})_c, \tag{B11}$$

$$\frac{\partial\delta n_{is}^{(g)}}{\partial t} - u_{i\|c} - \epsilon u_{i\|0} = i(k_r a_i q)[\delta p_{i\|0} + \delta p_{i\perp 0} + \phi_0 e^{-b_i/2}\times(2-b_i/2)] + (\mathcal{N}_{i0})_s,$$

the parallel ion momentum balance equations,

$$\frac{\partial u_{i\|0}}{\partial t} + \frac{\epsilon}{2}(\delta p_{i\perp s} - \delta p_{i\|s}) = \frac{i}{2}(k_r a_i q)(q_{i\|s} + q_{i\perp s} + 4u_{i\|s}) + \frac{\epsilon}{4}\phi_s b_i e^{-b_i/2} + (\mathcal{N}_{i1})_0,$$

$$\frac{\partial u_{i\|c}}{\partial t} + \delta p_{i\|s} = -\phi_s e^{-b_i/2} + (\mathcal{N}_{i1})_c, \tag{B12}$$

$$\frac{\partial u_{i\|s}}{\partial t} - \delta p_{i\|c} + \epsilon(\delta p_{i\perp 0} - \delta p_{i\|0}) = i(k_r a_i q)(q_{i\|0} + q_{i\perp 0} + 4u_{i\|0}) + e^{-b_i/2}\left(\phi_c + \frac{\epsilon}{2}\phi_0 b_i\right) + (\mathcal{N}_{i1})_s,$$

the perturbed parallel ion pressure equations,

$$\frac{\partial\delta p_{i\|0}}{\partial t} + \frac{\epsilon}{2}(2q_{i\perp s} - q_{i\|s} - u_{i\|s}) = \frac{i}{2}(k_r a_i q)[\delta r_{i\|\|s} + \delta r_{i\|\perp s} + \phi_s e^{-b_i/2}(4-b_i/2)] + (\mathcal{N}_{i2\|})_0,$$

$$\frac{\partial\delta p_{i\|c}}{\partial t} + q_{i\|s} + 3u_{i\|s} = (\mathcal{N}_{i2\|})_c, \tag{B13}$$

$$\frac{\partial\delta p_{i\|s}}{\partial t} - q_{i\|c} - 3u_{i\|c} + \epsilon(2q_{i\perp 0} - q_{i\|0} - u_{i\|0}) = i(k_r a_i q)[\delta r_{i\|\|0} + \delta r_{i\|\perp 0} + \phi_0 e^{-b_i/2}(4-b_i/2)] + (\mathcal{N}_{i2\|})_s,$$

the perturbed perpendicular ion pressure equations,

$$\frac{\partial \delta p_{i\perp 0}}{\partial t} - \epsilon(q_{i\perp s} + u_{i\parallel s}) = \frac{i}{2}(k_r a_i q)[\delta r_{i\parallel\perp s} + \delta r_{i\perp\perp s} + \phi_s e^{-b_i/2} \times (3 - 3b_i/2 + b_i^2/8)] + (\mathcal{N}_{i2\perp})_0,$$

$$\frac{\partial \delta p_{i\perp c}}{\partial t} + q_{i\perp s} + u_{i\parallel s} = (\mathcal{N}_{i2\perp})_c, \quad \text{(B14)}$$

$$\frac{\partial \delta p_{i\perp s}}{\partial t} - q_{i\perp c} - u_{i\parallel c} - 2\epsilon(q_{i\perp 0} + u_{i\parallel 0}) = i(k_r a_i q)[\delta r_{i\parallel\perp 0} + \delta r_{i\perp\perp 0} + \phi_0 e^{-b_i/2} \times (3 - 3b_i/2 + b_i^2/8)] + (\mathcal{N}_{i2\perp})_s,$$

and the quasineutrality conditions,

$$e^{-b_i/2}\left(\delta n_{i0}^{(g)} - \frac{b_i}{2}\delta T_{i\perp 0}\right) - \phi_0[1 - \Gamma_0(b_i)] = -\frac{\epsilon}{2\tau_e}\phi_c,$$

$$e^{-b_i/2}\left(\delta n_{ic}^{(g)} - \frac{b_i}{2}\delta T_{i\perp c}\right) - \phi_c[1 - \Gamma_0(b_i)] = \frac{1}{\tau_e}\phi_c, \quad \text{(B15)}$$

$$e^{-b_i/2}\left(\delta n_{is}^{(g)} - \frac{b_i}{2}\delta T_{i\perp s}\right) - \phi_s[1 - \Gamma_0(b_i)] = \frac{1}{\tau_e}\phi_s,$$

where the closure relations for the parallel ion heat fluxes $q_{i\parallel} = q_{i\parallel}^{(l)} + q_{i\parallel}^{(s)}$ and $q_{i\perp} = q_{i\perp}^{(l)} + q_{i\perp}^{(s)}$ are given by

$$q_{i\parallel 0}^{(l)} = -2q_{i\perp 0}^{(l)} = 2U_i\left(1 - \frac{\hat{\beta}_2}{\hat{\beta}_1}\right),$$

$$q_{i\parallel c}^{(l)} = -2q_{i\perp c}^{(l)} = 2\epsilon U_i\left(-1 + 2\frac{\hat{\beta}_2}{\hat{\beta}_1}\right),$$

$$U_i = \hat{\beta}_1(\hat{\beta}_1 - 1)^{-1} \times \left(u_{i\parallel 0} + \epsilon u_{i\parallel c} - u_{i\parallel 0}(t=0) - \int_0^t dt' \mathcal{N}_{i10}(t')\right),$$

$$q_{i\parallel c}^{(s)} = -2\sqrt{2/\pi}\,\delta T_{i\parallel s},$$

$$q_{i\parallel s}^{(s)} = 2\sqrt{2/\pi}\,\delta T_{i\parallel c}, \quad \text{(B16)}$$

$$q_{i\perp c}^{(s)} = -\sqrt{2/\pi}\,\delta T_{i\perp s},$$

$$q_{i\perp s}^{(s)} = \sqrt{2/\pi}\,\delta T_{i\perp c},$$

$$q_{i\parallel s}^{(l)} = q_{i\perp s}^{(l)} = q_{i\parallel 0}^{(s)} = q_{i\perp 0}^{(s)} = 0$$

and the $(0,c,s)$ components of the fourth-order ion fluid variables $(\delta r_{i\parallel\parallel}, \delta r_{i\parallel\perp}, \delta r_{i\perp\perp})$ are immediately written in terms of $(\delta n_{i\parallel 0}^{(g)}, \delta n_{i\parallel c}^{(g)}, \delta n_{i\parallel s}^{(g)})$ by using Eq. (B8).

APPENDIX C: KINETIC-FLUID EQUATIONS OF ETG-MODE-DRIVEN ZONAL FLOWS IN LARGE-ASPECT-RATIO TOKAMAKS

In the same manner as in Appendix B, the kinetic-fluid equations of ETG-mode-driven zonal flows for large-aspect-ratio tokamaks are considered here. In this Appendix, we assume the long radial wavelength $a_i^{-1} \ll k_\perp < a_e^{-1}$ and use the following normalization:

$$\left[\frac{v_{te}t}{R_0 q}, \frac{e\phi_{\mathbf{k}_\perp}}{T_e}, \frac{\delta n_{e\mathbf{k}_\perp}^{(g)}}{n_0}, \frac{u_{e\parallel\mathbf{k}_\perp}}{v_{te}}, \frac{\delta p_{e\parallel\mathbf{k}_\perp}}{p_{e0}}, \frac{\delta p_{e\perp\mathbf{k}_\perp}}{p_{e0}}\right] \to [t, \phi, \delta n_e^{(g)}, u_{e\parallel}, \delta p_{e\parallel}, \delta p_{e\perp}],$$

$$\left[\frac{q_{e\parallel\mathbf{k}_\perp}}{p_{e0}v_{te}}, \frac{q_{e\perp\mathbf{k}_\perp}}{p_{e0}v_{te}}, \frac{\delta r_{e\parallel\parallel\mathbf{k}_\perp}}{p_{e0}v_{te}^2}, \frac{\delta r_{e\parallel\perp\mathbf{k}_\perp}}{p_{e0}v_{te}^2}, \frac{\delta r_{e\perp\perp\mathbf{k}_\perp}}{p_{e0}v_{te}^2}\right] \to [q_{e\parallel}, q_{e\perp}, \delta r_{e\parallel\parallel}, \delta r_{e\parallel\perp}, \delta r_{e\perp\perp}], \quad \text{(C1)}$$

$$\left[\frac{R_0 q \mathcal{N}_{e0\mathbf{k}_\perp}}{n_0 v_{te}}, \frac{R_0 q \mathcal{N}_{e1\mathbf{k}_\perp}}{p_{e0}}, \frac{R_0 q \mathcal{N}_{e2\parallel\mathbf{k}_\perp}}{p_{e0}v_{te}}, \frac{R_0 q \mathcal{N}_{e2\perp\mathbf{k}_\perp}}{p_{e0}v_{te}},\right] \to [\mathcal{N}_{e0}, \mathcal{N}_{e1}, \mathcal{N}_{e2\parallel}, \mathcal{N}_{e2\perp}]$$

where $v_{te} \equiv (T_e/m_e)^{1/2}$. Then, replacing the normalized potential ϕ, the subscript i, and the thermal gyroradius a_i for ions with $(-\phi)$, e, and $(-a_e)$, respectively, everywhere in Eqs. (B2)–(B5), (B7), and (B8), we immediately obtain corresponding electron fluid equations of the perturbed gyrocenter density, the parallel momentum balance, the perturbed parallel pressure, the perturbed perpendicular pressure, the parallel heat fluxes, and the fourth-order variables. Poisson's equation relevant to the case of ETG turbulence is written as

$$e^{-b_e/2}\left(\delta n_e^{(g)} - \frac{b_e}{2}\delta T_{e\perp}\right) + \phi[\tau_e + 1 - \Gamma_0(b_e) + k_r^2 \lambda_{\mathrm{De}}^2] = 0, \quad \text{(C2)}$$

where $\tau_e \equiv T_e/T_i$, $b_e \equiv k_r^2 a_e^2$, $a_e \equiv v_{te}/|\Omega_{e0}|$, and $\Omega_{e0} \equiv -eB_0/(m_e c)$.

Further simplifications are done by neglecting $\mathcal{O}(\epsilon^2)$ terms and assuming in the same way as in Eq. (B9) that the poloidal-angle dependence of an arbitrary fluid variable consists of constant, cosine, and sine parts, which are denoted by the subscripts 0, c, and s, respectively. Then, the electron version of Eqs. (B11)–(B14) and (B16) are easily obtained by replacing again the normalized potential ϕ, the subscript i, and the thermal gyroradius a_i with $(-\phi)$, e, and $(-a_e)$, respectively, there. Also, derivation of the $(0,c,s)$ components of Poisson's equation, Eq. (C2), is trivial.

APPENDIX D: DERIVATION OF THE GAM DISPERSION RELATION FROM KINETIC-FLUID EQUATIONS

In this Appendix, the GAM dispersion relation is derived from the kinetic-fluid equations in Appendix B. Here, in order to obtain the frequency and the damping rate for a short-time GAM oscillation-damping process through which an initial zonal-flow perturbation evolves into the steady solution (or the residual zonal flow), we use Eqs. (B11)–(B16) with both the long-time (or steady) solution part and the nonlinear terms neglected. We also put

$$\delta n_{ic}^{(g)} = \phi_c = u_{i\|0} = u_{i\|s} = \delta p_{i\|0} = \delta p_{i\|c} = \delta p_{i\perp 0} = \delta p_{i\perp c} = 0 \tag{D1}$$

for the GAM oscillations and replace $\partial/\partial t$ with $-i\omega$ in Eqs. (B11)–(B14) to obtain linear equations written as

$$\begin{bmatrix} \omega & \frac{1}{2}q^2 & \frac{1}{2}q^2 & 0 & \tau_e q^2 \\ 4 & (\omega+i\chi_1) & 0 & 3 & -i\chi_1 \\ 3 & 0 & (\omega+i\chi_2) & 1 & -i\chi_2 \\ 0 & 1 & 0 & \omega & \tau_e \\ 2 & 0 & 0 & 1 & \omega \end{bmatrix} \begin{bmatrix} \phi_0 \\ \delta p_{i\|s}/(k_r a_i q) \\ \delta p_{i\perp s}/(k_r a_i q) \\ -iu_{i\|c}/(k_r a_i q) \\ \delta n_{is}^{(g)}/(k_r a_i q) \end{bmatrix} = 0, \tag{D2}$$

where $\chi_1 \equiv 2\sqrt{2/\pi}$ and $\chi_2 \equiv \sqrt{2/\pi}$. Representing the 5×5 matrix in Eq. (D2) by M, the GAM dispersion relation is given by

$$\det M \equiv \omega^5 + c_1\omega^4 + c_2\omega^3 + c_3\omega^2 + c_4\omega + c_5 = 0, \tag{D3}$$

where

$$\begin{aligned} c_1 &= i(\chi_1+\chi_2), \\ c_2 &= -[q^2(7/2+2\tau_e) + 3 + \tau_e + \chi_1\chi_2], \\ c_3 &= -i[q^2\{\chi_1(5/2+2\tau_e) + \chi_2(3+2\tau_e)\} + \chi_1(1+\tau_e) \\ &\quad + \chi_2(3+\tau_e)], \\ c_4 &= q^2\{5/2 + 3\tau_e/2 + 2\chi_1\chi_2(1+\tau_e)\} + \chi_1\chi_2(1+\tau_e), \\ c_5 &= iq^2(\chi_1/2+\chi_2)(1+\tau_e). \end{aligned} \tag{D4}$$

Now, in order to analytically solve Eq. (D3), we assume the GAM phase velocity to be larger than the ion thermal velocity so that, in our dimensionless representation, $\omega \sim q > 1$ which is examined later from the final result. Then, Eq. (D3) is rewritten as

$$q^{-5}\det M = \left(\frac{\omega}{q}\right)^5 - \left(\frac{7}{2}+2\tau_e\right)\left(\frac{\omega}{q}\right)^3 + \frac{i}{q}\left[(\chi_1+\chi_2) \times \left(\frac{\omega}{q}\right)^4 - \left\{\chi_1\left(\frac{5}{2}+2\tau_e\right) + \chi_2(3+2\tau_e)\right\} \times \left(\frac{\omega}{q}\right)^2\right] = 0, \tag{D5}$$

where small terms of $\mathcal{O}(q^{-2})$ are neglected. Solving Eq. (D5) for ω/q up to $\mathcal{O}(q^{-1})$, we finally obtain the approximate expression of the GAM dispersion relation as

$$\frac{\omega}{q} = \pm\sqrt{\frac{7+4\tau_e}{2}} - \frac{i}{q}\left(\frac{\chi_1+\chi_2/2}{7+4\tau_e}\right), \tag{D6}$$

which is represented in the physical dimensional form by

$$\omega = \frac{v_{ti}}{R_0}\left[\pm\sqrt{\frac{7+4\tau_e}{2}} - \frac{i}{q}\left(\frac{\chi_1+\chi_2/2}{7+4\tau_e}\right)\right]. \tag{D7}$$

We now confirm the aforementioned assumption that the ratio of the GAM phase velocity to the ion thermal velocity is scaled with q such that $R_0 q\omega/v_{ti} \sim q$. The real frequency in Eq. (D7), which contains a different numerical factor from the one derived from the MHD model,[3] is the same as that derived from the kinetic model[9,21–23] up to $\mathcal{O}(q^{-1})$. However, the damping rate in Eq. (D7) is not the same as the kinetic result because, in deriving the dissipative part of the parallel heat fluxes given by Eq. (61), the resonant ions' population is evaluated not by using the correct phase velocity but by taking the adiabatic limit in which the parallel velocity of the resonant ions is regarded as negligibly small compared with the ion thermal velocity.

1. P. H. Diamond, S.-I. Itoh, K. Itoh, and T. S. Hahm, Plasma Phys. Controlled Fusion **47**, R35 (2005).
2. K. Itoh, S.-I. Itoh, P. H. Diamond, T. S. Hahm, A. Fujisawa, G. R. Tynan, M. Yagi, and Y. Nagashima, Phys. Plasmas **13**, 055502 (2006).
3. N. Winsor, J. L. Johnson, and J. J. Dawson, Phys. Fluids **11**, 2248 (1968).
4. A. Fujisawa, K. Itoh, H. Iguchi, *et al.*, Phys. Rev. Lett. **93**, 165002 (2004).
5. G. D. Conway, B. Scott, J. Schirmer, M. Reich, A. Kendl, and the ASDEX Upgrade Team, Plasma Phys. Controlled Fusion **47**, 1165 (2005).
6. W. Horton, Rev. Mod. Phys. **71**, 735 (1999).
7. M. N. Rosenbluth and F. L. Hinton, Phys. Rev. Lett. **80**, 724 (1998).
8. H. Sugama and T.-H. Watanabe, Phys. Rev. Lett. **94**, 115001 (2005).
9. H. Sugama and T.-H. Watanabe, Phys. Plasmas **13**, 012501 (2006).
10. A. M. Dimits, G. Bateman, M. A. Beer, *et al.*, Phys. Plasmas **7**, 969 (2000).
11. T.-H. Watanabe and H. Sugama, Nucl. Fusion **46**, 24 (2006).
12. M. A. Beer and G. W. Hammett, *Proceedings of the Joint Varenna-Lausanne International Workshop on Theory of Fusion Plasmas*, Varenna, 1998, edited by J. W. Connor *et al.* (Societa Italiana de Fisca, Bologna, Italy, 1999), p. 19.
13. F. Jenko and W. Dorland, Phys. Rev. Lett. **89**, 225001 (2002).
14. E. Kim, C. Holland, and P. H. Diamond, Phys. Rev. Lett. **91**, 075003 (2003).
15. H. Sugama, T.-H. Watanabe, and W. Horton, Phys. Plasmas **8**, 2617 (2001).
16. H. Sugama, T.-H. Watanabe, and W. Horton, Phys. Plasmas **10**, 726 (2003).
17. G. W. Hammett and F. W. Perkins, Phys. Rev. Lett. **64**, 3019 (1990).
18. E. A. Frieman and L. Chen, Phys. Fluids **25**, 502 (1982).
19. R. D. Hazeltine and J. D. Meiss, *Plasma Confinement* (Addison-Wesley, Redwood City, 1992), p. 298.
20. R. L. Dewar and A. H. Glasser, Phys. Fluids **26**, 3038 (1983).
21. H. Sugama and T.-H. Watanabe, J. Plasma Phys. **72**, 825 (2006).
22. V. B. Lebedev, P. N. Yushmanov, P. H. Diamond, S. V. Novakovskii, and A. I. Smolyakov, Phys. Plasmas **3**, 3023 (1996).
23. S. V. Novakovskii, C. S. Liu, R. Z. Sagdeev, and M. N. Rosenbluth, Phys. Plasmas **4**, 4272 (1997).
24. Z. Lin, T. S. Hahm, W. W. Lee, W. M. Tang, and R. B. White, Phys. Plasmas **7**, 1857 (2000).
25. S. P. Hirshman, Nucl. Fusion **18**, 917 (1978).